Received: 11 August 2022 | Revised: 29 December 2022 | Accepted: 27 January 2023
DOI: 10.1002/asmb.2749

RESEARCH ARTICLE

WILEY

A new Wiener process with bathtub-shaped degradation rate in the presence of random effects

Massimiliano Giorgio[1] | **Antonio Piscopo**[2] | **Gianpaolo Pulcini**[3]

[1]Dipartimento di Ingegneria Industriale, Università di Napoli Federico II, Naples, Italy

[2]Scuola Superiore Meridionale, Naples, Italy

[3]Istituto Scienze e Tecnologie per Energia e Mobilità Sostenibili (STEMS), CNR, Naples, Italy

Correspondence
Massimiliano Giorgio, Dipartimento di Ingegneria Industriale, Università di Napoli Federico II, P.le V. Tecchio 80, 80125 Napoli (NA), Naples, Italy.
Email: massimiliano.giorgio@unina.it

Funding information
Universita degli Studi di Napoli Federico II within the CRUI-CARE Agreement

Abstract

This paper proposes a new time scaled Wiener process with random effects that has been specially designed to allow the description of non-monotonic degradation phenomena with bathtub shaped degradation rate, here intended as derivative of the mean function. Two different parameterizations of the proposed Wiener process are suggested, and the main features of the process are illustrated and discussed. The maximum likelihood estimation of its parameters is addressed. A failure threshold model is adopted to formulate and estimate the probability distribution function of the remaining useful life, which constitutes the core prognostic tool in condition-based maintenance. As a motivating example, the proposed model is applied to a set of real degradation data of metal-oxide-semiconductor field-effect transistors, where, as a result of preliminary analyses, some of the process parameters are assumed to be random in order to describe the considerable heterogeneity observed between the degradation paths of different units. Obtained results demonstrate the affordability and utility of the proposed model, especially for the estimation of unit-specific features performed on the basis of degradation data collected in the early phase of the life of a unit belonging to the considered heterogeneous population.

KEYWORDS

bathtub shaped degradation rate, estimation of unit-specific features from early data, random effects, remaining useful life, time-scaled Wiener process

1 | INTRODUCTION

The most of gamma, inverse Gaussian and Wiener based degradation models proposed in the literature (see, e.g., Abdel-Hameed,[1] van Noortwijk,[2] Ye & Chen,[3] Whitmore and Schenkelberg,[4] Wang,[5] Wang & Xu,[6] Ye et al.,[7] and Kahle et al.[8]) are characterized by a monotonic degradation rate function, here intended as the derivative of the mean degradation function. However, the degradation mean function of technological units is often inverse S-shaped, and hence the degradation rate function is typically bathtub-shaped. In fact, real world degradation processes generally present three phases: a first phase where the degradation rate function presents a decreasing behavior, a second phase where it is almost constant, and a third phase where it increases. These three phases are usually referred to as accommodation phase, steady state (or normal) phase, and degenerative (or catastrophic) phase, respectively (see, e.g., Gertsbakh and Kordonskiy[9]).

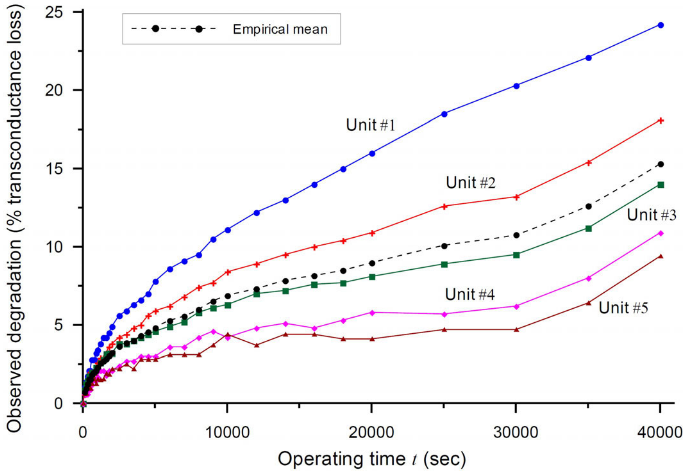

FIGURE 1 The degradation paths (in percent transconductance loss) and the empirical mean of the five MOSFETs (data pertaining to the same degradation path are connected by lines to improve readability)

Models with monotonic degradation rate function are clearly able to describe only two of these three phases. On the other side, these models are usually applied to sets of degradation data that do not exhibit all of the mentioned three phases. This is not the case of the set of real degradation data of metal-oxide-semiconductor field-effect transistors (MOSFETs) displayed in Figure 1, which gives clear evidence that the empirical mean function of the observed degradation process (see the black dashed line) is inverse S-shaped, so that the degradation rate function is bathtub-shaped.

Nonetheless, at the best of the authors knowledge, the only example of continuous-time, continuous-state degradation process with bathtub degradation rate function is provided by Peng et al.[10] who proposed a 3-parameter inverse S-shaped mean function, both for the Inverse Gaussian process and for the competing gamma and Wiener processes considered in the same paper for comparative purposes.

An alternative strategy for modeling the degradation data reported in Figure 1 is suggested in Chen et al.[11] where the bathtub shaped behavior of the degradation rate function is modeled by adopting a change point approach. This approach, which is commonly adopted to describe degradation phenomena where the degradation rate and/or other characteristics of the degradation phenomenon of interest change abruptly at a given change-point, consists in using different models to describe the evolution of the degradation process before and after the change point (see, e.g., Wang et al.,[12] Kong et al.,[13] Liu et al.,[14] Gao et al.,[15] and Lin et al.[16]). A limitation of this method is that the resulting whole model is usually indexed by a large number of parameters. In addition, the model parameters are estimated by adopting cumbersome procedures that, to put it simply, consist in detecting the location of the change point by means of semi-heuristic algorithms and in estimating the parameters of the model used in a given phase from the data collected in that phase only. As a consequence, by using such a change-point approach, it is very difficult, if not impossible, to make inference on the residual reliability and/or on the remaining useful life when the most of available data are collected during the early phase or just after the change-point.

Motivated by the mentioned arguments, in this paper we propose and apply to the MOSFET data a new time scaled Wiener process (see, e.g., Whitmore and Schenkelberg[4] and Wang[5]) with random effect that can describe degradation phenomena where the degradation rate function is bathtub-shaped. An important characteristic of the proposed model is that it can be used to make inference on features of a (new) unit belonging to the considered heterogeneous population also from data collected only in the early phase of its life. Obtained results show that the proposed model fits adequately the MOSFET data and demonstrates the effectiveness and affordability of the proposed approach.

The paper is organized as it follows. Section 2 introduces the proposed Wiener process in its basic form and illustrates its main features. In particular, two different parameterizations of the proposed WP are formulated, which allows describing different forms of unit-to-unit variability and (hence) accounting for the presence of different forms of heterogeneities. The remaining useful life of the units and its probability distribution are here defined and formulated, by adopting a failure threshold model. Section 3 discusses the maximum likelihood estimation of the parameters of the basic model. Section 4 is devoted to the analysis of the MOSFET data. In this section, a preliminary analysis is performed that gives evidence of the presence of form of heterogeneity among the degradation paths of the different units. Hence, in order to account for this form of (unit-to-unit) variability, the basic model is extended to incorporate random effects. This extended version of the proposed new time scaled Wiener model is then applied to the MOSFET data. Finally, Section 5 is devoted to final considerations.

2 | THE PROPOSED WIENER PROCESS

The aim of this paper is proposing a new characterization of the time scaled Wiener process (WP) that can describe degradation phenomena where the degradation rate function is bathtub-shaped. The time scaled Wiener process $\{W(t), t \geq 0\}$ is a stochastic process with independent, non-stationary, and Gaussian distributed increments, that can be defined as:

$$W(t) = \Lambda(t) + \sigma_0 B(\Lambda(t)), \tag{1}$$

where $\{B(t), t \geq 0\}$ is the standard Brownian motion, $\sigma_0 > 0$ is the diffusion coefficient, and $\Lambda(t)$ is a monotonic increasing function, which represents the mean function of the process, $E\{W(t)\}$. In this paper, by degradation rate function we intend the first derivative of $\Lambda(t)$ with respect to t.

The proposed model is obtained by assigning to $\Lambda(t)$ (and hence to $E\{W(t)\}$) the following 4-parameter expression:

$$\Lambda(t) = E\{W(t)\} = (t/\alpha_1)^{\beta_1} + (t/\alpha_2)^{\beta_2}, \tag{2}$$

where α_1, α_2, β_1, and β_2 are positive valued parameters. As requested, the resulting time scaled WP can describe (among the others) phenomena where the degradation rate function is bathtub shaped. In fact, under the proposed model, the degradation rate function has the following expression:

$$\frac{\mathrm{d}\Lambda(t)}{\mathrm{d}t} = \frac{\mathrm{d}E\{W(t)\}}{\mathrm{d}t} = \frac{\beta_1}{\alpha_1}\left(\frac{t}{\alpha_1}\right)^{\beta_1-1} + \frac{\beta_2}{\alpha_2}\left(\frac{t}{\alpha_2}\right)^{\beta_2-1}, \tag{3}$$

which is bathtub shaped, provided that $(\beta_1 - 1)\,/\,(\beta_2 - 1) < 0$. It is worth to note that the degradation rate function (3) has the same functional form of the bathtub shaped hazard function suggested in Xie and Lai.[17] Indeed, alternative bathtub shaped characterizations of the time scaled WP can be readily obtained by assigning to the degradation rate function $\mathrm{d}\Lambda(t)/\mathrm{d}t$ functional forms that coincide with other bathtub shaped hazard functions proposed in the literature (see Lai et al.[18] and Nadarajah[19] for a review of existing models).

From (3), being:

$$\frac{\mathrm{d}^2E\{W(t)\}}{\mathrm{d}t^2} = \frac{\beta_1\,(1-\beta_1)}{\alpha_1^2}\left(\frac{t}{\alpha_1}\right)^{\beta_1-2} + \frac{\beta_2\,(1-\beta_2)}{\alpha_2^2}\left(\frac{t}{\alpha_2}\right)^{\beta_2-2}, \tag{4}$$

the inflection point t_{infl} of the mean function, that is, the time at which the degradation rate function reaches its minimum and $\mathrm{d}^2E\{W(t)\}/\mathrm{d}t^2 = 0$, is located at:

$$t_{infl} = \left[-\frac{\beta_2\,(\beta_2-1)}{\beta_1\,(\beta_1-1)}\,\frac{\alpha_1^{\beta_1}}{\alpha_2^{\beta_2}}\right]^{1/(\beta_1-\beta_2)}. \tag{5}$$

In Figure 2 the degradation mean of the proposed WP is depicted for selected parameters $(\alpha_2, \beta_1, \beta_2)$ and common inflection point, say $t_{infl} = 50$. In the cases considered in this figure, the inequality $(\beta_1 - 1)\,/\,(\beta_2 - 1) < 0$ is always satisfied. Moreover, in order that $t_{infl} = 50$, the scale parameter α_1 is set to:

$$\alpha_1 = \left[-50^{\beta_1-\beta_2}\,\alpha_2^{\beta_2}\,\frac{\beta_1\,(\beta_1-1)}{\beta_2\,(\beta_2-1)}\right]^{1/\beta_1}. \tag{6}$$

Figure 3 shows the degradation rate functions corresponding to the mean functions represented in Figure 2, which confirm the ability of the proposed model to describe different bathtub behaviors and give evidence of the flexibility of the proposed model.

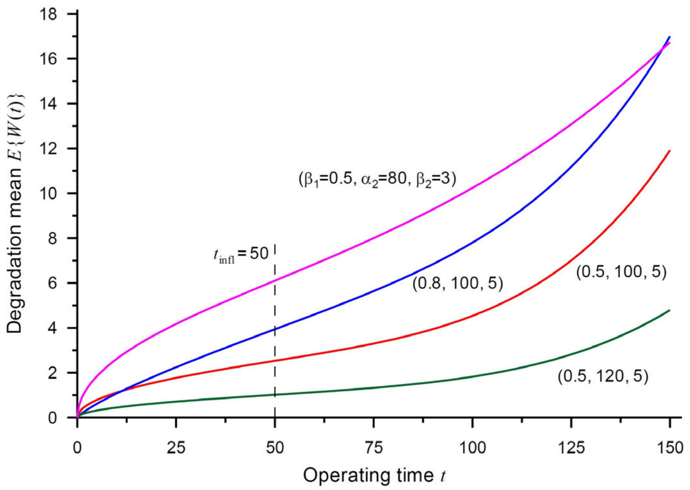

FIGURE 2 Shapes of the mean function of proposed WP with different values of process parameters and common inflection point $t_{infl} = 50$

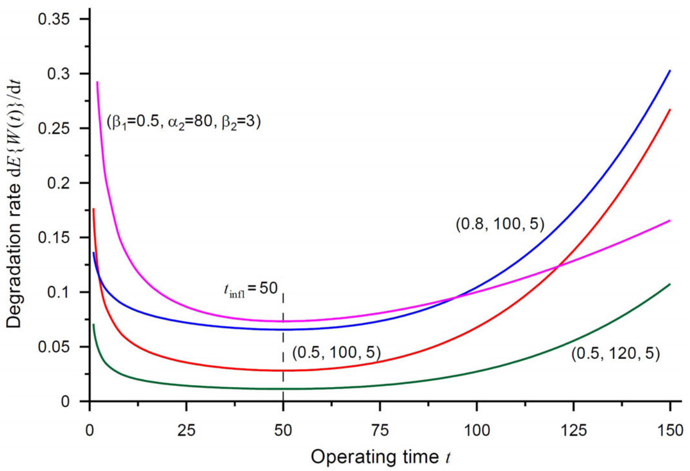

FIGURE 3 Shapes of the degradation rate function of the proposed WP with different values of process parameters and common inflection point $t_{infl} = 50$

Given an initial condition, the proposed time scaled WP is fully defined by the probability density function (pdf) of the degradation increment $\Delta W(t, \Delta t)$ during the time interval $(t, t + \Delta t)$. This pdf can be expressed as:

$$f_{\Delta W(t,\Delta t)}(\delta) = \frac{1}{\sqrt{2\pi\ \sigma_0^2\ \Delta\Lambda(t, \Delta t)}} \exp\left[-\frac{1}{2}\ \frac{(\delta - \Delta\Lambda(t, \Delta t))^2}{\sigma_0^2\ \Delta\Lambda(t, \Delta t)}\right], -\infty < \delta < \infty, \tag{7}$$

where $\sigma_0 > 0$ is the diffusion coefficient, $\Lambda(t)$ is the mean function (2), and $\Delta\Lambda(t, \Delta t) = \Lambda(t + \Delta t) - \Lambda(t)$.

From (7), and the corresponding cumulative distribution function (Cdf) of the degradation increment is given by:

$$F_{\Delta W(t,\Delta t)}(\delta) = \Phi\left(\frac{\delta - \Delta\Lambda(t, \Delta t)}{\sigma_0\sqrt{\Delta\Lambda(t, \Delta t)}}\right), \tag{8}$$

where $\Phi(\cdot)$ denotes the standard normal Cdf.

The variance function of the process is given by:

$$V\{W(t)\} = \sigma_0^2\, \Lambda(t) = \sigma_0^2 \left[\left(\frac{t}{\alpha_1}\right)^{\beta_1} + \left(\frac{t}{\alpha_2}\right)^{\beta_2} \right], \tag{9}$$

and the variance-to-mean ratio $V\{W(t)\}/E\{W(t)\}$ is constant with the operating time and equal to the squared diffusion coefficient σ_0^2.

An alternative parameterization of the proposed WP is given by:

$$W(t) = \mu\, \Lambda^*(t) + \sigma B\left(\Lambda^*(t)\right), \tag{10}$$

where $\Lambda^*(t) = t^{\beta_1} + (t/\alpha)^{\beta_2}$, $\mu, \alpha, \beta_1, \beta_2, \sigma > 0$, and $(\beta_1 - 1)/(\beta_2 - 1) < 0$. This alternative parameterization has been obtained from (1) and (2) by setting $\mu = (1/\alpha_1)^{\beta_1}$, $\alpha = \alpha_2/\alpha_1^{\beta_1/\beta_2}$, and $\sigma = \sigma_0/\alpha_1^{\beta_1/2}$.

The pdf of the degradation increment $\Delta W(t, \Delta t)$ under this alternative parameterization is given by:

$$f_{\Delta W(t,\Delta t)}(\delta) = \frac{1}{\sqrt{2\pi\, \sigma^2 \Delta\Lambda^*(t, \Delta t)}} \exp\left[-\frac{1}{2} \frac{(\delta - \mu\, \Delta\Lambda^*(t, \Delta t))^2}{\sigma^2 \Delta\Lambda^*(t, \Delta t)} \right], \quad -\infty < \delta < \infty, \tag{11}$$

where $\Delta\Lambda^*(t, \Delta t) = \Lambda^*(t + \Delta t) - \Lambda^*(t)$. The mean $E\{W(t)\}$ and variance $V\{W(t)\}$ functions of the degradation process (10) are given by, respectively:

$$E\{W(t)\} = \mu\, \left[t^{\beta_1} + (t/\alpha)^{\beta_2}\right], \tag{12}$$

$$V\{W(t)\} = \sigma^2 \left[t^{\beta_1} + (t/\alpha)^{\beta_2}\right], \tag{13}$$

and the (constant) variance-to-mean ratio is now equal to σ^2/μ. Obviously, it is $\sigma^2/\mu = \sigma_0^2$.

Finally, under this alternative parameterization, the degradation rate function $\mathrm{d}\Lambda^*(t)/\mathrm{d}t$ is given by:

$$\frac{\mathrm{d}\Lambda^*(t)}{\mathrm{d}t} = \beta_1 t^{\beta_1 - 1} + \left(\frac{\beta_2}{\alpha}\right) \left(\frac{t}{\alpha}\right)^{\beta_2 - 1}$$

and the inflection point t_{infl} of the mean curve, which in this case depends only on three process parameters, say α, β_1, and β_2, is located at:

$$t_{infl} = \left[-\frac{\beta_2\,(\beta_2 - 1)}{\beta_1\,(\beta_1 - 1)} \frac{1}{\alpha^{\beta_2}} \right]^{1/(\beta_1 - \beta_2)}. \tag{14}$$

It is useful to remark that, considering alternative parameterizations of the proposed WP in the absence of unit-to-unit variability does not give any advantages in term of fitting ability of the model. On the contrary, when some parameters are unit-specific, different parameterizations can be useful for describing different forms of heterogeneity.

2.1 | Remaining useful life and reliability

Degrading units are usually assumed to fail when their degradation level passes an assigned failure threshold, say D. More precisely, when the underling degradation process is non monotonic, the unit lifetime X is defined as the first passage time of the hidden degradation process to D:

$$X = \inf\{x : W(x) > D\} \tag{15}$$

and the remaining useful life (RUL) X_t, at the current time t, is defined as

$$X_t = \max\{0, X - t\}, \tag{16}$$

so that, X_t is equal to $X - t$ if the unit at t is unfailed, and is assumed to be 0 otherwise.

From Giorgio and Pulcini,[20] the conditional pdf and Cdf of the RUL under the proposed WP (1) with bathtub shaped degradation rate function, given the degradation level w_t at the current time t, are respectively given by:

$$f_{X_t}(x|w_t) = \frac{D - w_t}{\sqrt{2\pi\,\sigma_0^2\,[\Delta\Lambda(t,x)]^3}} \exp\left[-\frac{1}{2}\frac{(D - w_t - \Delta\Lambda(t,x))^2}{\sigma_0^2\,\Delta\Lambda(t,x)}\right]\frac{\mathrm{d}\Delta\Lambda(t,x)}{\mathrm{d}x}, \quad x \geq 0, \tag{17}$$

and

$$F_{X_t}(x|w_t) = \Phi\left(\sqrt{\frac{\lambda}{\Delta\Lambda(t,x)}}\left(\frac{\Delta\Lambda(t,x)}{D - w_t} - 1\right)\right) + \exp\left[\frac{2\,(D - w_t)}{\sigma_0^2}\right]\Phi\left(-\sqrt{\frac{\lambda}{\Delta\Lambda(t,x)}}\left(\frac{\Delta\Lambda(t,x)}{D - w_t} + 1\right)\right), \tag{18}$$

where $\lambda = (D - w_t)^2/\sigma_0^2$ and, from (2):

$$\frac{\mathrm{d}\Delta\Lambda(t,x)}{\mathrm{d}x} = \frac{\beta_1}{\alpha_1}\left(\frac{t+x}{\alpha_1}\right)^{\beta_1 - 1} + \frac{\beta_2}{\alpha_2}\left(\frac{t+x}{\alpha_2}\right)^{\beta_2 - 1}. \tag{19}$$

Details about the derivation of these functions in the case of the basic Wiener process (i.e., when $\Lambda(t,x) \propto x$) are given in Kahle et al.[8]

From (17), the conditional mean RUL is given by:

$$E\{X_t|w_t\} = \int_0^{\infty} x\, f_{X_t}(x|w_t)\,\mathrm{d}x \tag{20}$$

and the conditional reliability function is $R_{X_t}(x|w_t) = 1 - F_{X_t}(x|w_t)$.

In computing the distribution of X_t, we have implicitly assumed that, if the degradation level at the time t is below the threshold limit D, then the probability that the process has passed this threshold before t is null. In fact, this assumption works quite satisfactorily when the mean of the increment is relatively large with respect to its standard deviation (a circumstance that often occurs in the case of real degradation processes). Note that, under this assumption, since the WP is Markovian, the conditional pdf (17) and Cdf (18), given $W(t) = w_t$, are independent of the past history of the process, depending only on the current degradation level w_t.

From (17) and (18), by setting $w_t = 0$ and $t = 0$, so that $\Delta\Lambda(0,x) \equiv \Lambda(x)$ and $\sqrt{\lambda} = D/\sigma_0$, the pdf and the Cdf of the useful life X of a new unit are given by:

$$f_X(x) = \frac{D}{\sqrt{2\pi\,\sigma_0^2\,[\Lambda(x)]^3}} \exp\left[-\frac{1}{2}\frac{(D - \Lambda(x))^2}{\sigma_0^2\,\Lambda(x)}\right]\frac{\mathrm{d}\Lambda(x)}{\mathrm{d}x}, x \geq 0, \tag{21}$$

and:

$$F_X(x) = \Phi\left(\frac{D}{\sigma_0}\sqrt{\frac{1}{\Lambda(x)}}\left(\frac{\Lambda(x)}{D} - 1\right)\right) + \exp\left(\frac{2\,D}{\sigma_0^2}\right)\Phi\left(-\frac{D}{\sigma_0}\sqrt{\frac{1}{\Lambda(x)}}\left(\frac{\Lambda(x)}{D} + 1\right)\right), \tag{22}$$

where $\mathrm{d}\Lambda(x)/\mathrm{d}x \equiv \mathrm{d}E\{W(t)\}/\mathrm{d}t$ is given in (3).

Clearly, all the above distributions can be expressed under the alternative parameterization (10) suggested at the end of the Section 1, by replacing $\mu\,\Lambda^*(x)$, $\mu\,\Delta\Lambda^*(t,x)$, and $\sigma/\sqrt{\mu}$ to $\Lambda(x)$, $\Delta\Lambda(t,x)$, and σ_0, respectively.

3 | THE LIKELIHOOD FUNCTION

Let us suppose that the degradation levels of m identical units that operate under identical operating conditions are recurrently observed at planned inspection epochs. Moreover, let n_i and $t_{i,1}, \ldots, t_{i,n_i}$ $(i = 1, \ldots, m)$ denote the number of inspections performed on the unit i and the corresponding inspection times, respectively.

Based on these data, under the basic WP (1), the log-likelihood function relative to the degrading unit i is given by:

$$\ell\,(\boldsymbol{\delta}_i) = -\frac{n_i}{2}\ln(2\pi) - n_i\,\ln(\sigma_0) - \frac{1}{2}\sum_{j=1}^{n_i}\ln\left(\Delta\Lambda_{i,j}\right) - \sum_{j=1}^{n_i}\frac{\left(\delta_{i,j}-\Delta\Lambda_{i,j}\right)^2}{2\,\sigma_0^2\,\Delta\Lambda_{i,j}}, \quad -\infty < \delta_{i,j} < \infty \tag{23}$$

where $\Delta\Lambda_{i,j} = \Delta\Lambda\left(t_{i,j-1}, t_{i,j} - t_{i,j-1}\right)$, $\delta_{i,j}$ is the observed degradation increment of the unit i during the j-th time interval $\left(t_{i,j-1}, t_{i,j}\right)$, with $t_{i,0} = 0$ for all i, and $\boldsymbol{\delta}_i = \left(\delta_{i,1}, \ldots, \delta_{i,n_i}\right)$ is the vector of the observed degradation increments of the unit i.

Consequently, from (23), the likelihood function relative to the m units results in:

$$\ell(\boldsymbol{\delta}) = -\frac{N}{2}\ln(2\pi) - N\,\ln(\sigma_0) - \frac{1}{2}\sum_{i=1}^{m}\sum_{j=1}^{n_i}\ln\left(\Delta\Lambda_{i,j}\right) - \sum_{i=1}^{m}\sum_{j=1}^{n_i}\frac{\left(\delta_{i,j}-\Delta\Lambda_{i,j}\right)^2}{2\,\sigma_0^2\,\Delta\Lambda_{i,j}}, \tag{24}$$

where $N = \sum_{i=1}^{m} n_i$ is the total number of observations and $\boldsymbol{\delta} = (\boldsymbol{\delta}_1, \ldots, \boldsymbol{\delta}_m)$ is the vector of all observed degradation increments.

The maximum likelihood (ML) estimates of $\alpha_1, \beta_1, \alpha_2, \beta_2$, and σ_0 are the values $\hat{\alpha}_1, \hat{\beta}_1, \hat{\alpha}_2, \hat{\beta}_2$, and $\hat{\sigma}_0$ that maximize the likelihood function (24). The ML estimate $\hat{\sigma}_0$ of σ_0 is given by:

$$\hat{\sigma}_0 = \sqrt{\frac{1}{N}\sum_{i=1}^{m}\sum_{j=1}^{n_i}\frac{\left(\delta_{i,j}-\widehat{\Delta\Lambda}_{i,j}\right)^2}{\widehat{\Delta\Lambda}_{i,j}}},$$

and depends on the ML estimates $\hat{\alpha}_1$, $\hat{\beta}_1$, $\hat{\alpha}_2$, and $\hat{\beta}_2$, of the parameters α_1, β_1, α_2, and β_2 through $\widehat{\Delta\Lambda}_{i,j} = \left(t_{i,j}/\hat{\alpha}_1\right)^{\hat{\beta}_1} + \left(t_{i,j}/\hat{\alpha}_2\right)^{\hat{\beta}_2} - \left(t_{i,j-1}/\hat{\alpha}_1\right)^{\hat{\beta}_1} - \left(t_{i,j-1}/\hat{\alpha}_2\right)^{\hat{\beta}_2}$. The ML estimates $\hat{\alpha}_1$, $\hat{\beta}_1$, $\hat{\alpha}_2$, and $\hat{\beta}_2$ are not available in closed form. However, they can be easily retrieved by using a numerical optimization method.

Clearly, due to the invariance property of the ML estimators, the ML estimates of the parameters μ, α, and σ under the alternative parameterization (10) proposed at the end of the Section 1 can be easily obtained from the ML estimates $\hat{\alpha}_1$, $\hat{\beta}_1$, $\hat{\alpha}_2$, $\hat{\beta}_2$, and $\hat{\sigma}_0$ as it follows: $\hat{\mu} = \left(1/\hat{\alpha}_1\right)^{\hat{\beta}_1}$, $\hat{\alpha} = \hat{\alpha}_2/\hat{\alpha}_1^{\hat{\beta}_1/\hat{\beta}_2}$, and $\hat{\sigma} = \hat{\sigma}_0/\hat{\alpha}_1^{\hat{\beta}_1/2}$.

4 | CASE STUDY

Let us consider the set of percent transconductance degradation data of some metal-oxide-semiconductor field-effect transistors (MOSFETs) reported in Table 1. These data were initially given in Lu et al.[21] and successively used in Yang[22] and Chen et al.[11] The dataset consists of 135 degradation measures of 5 MOSFETs. Specifically, there are 35 measures for each MOSFET, obtained at $n = 35$ measurement times, $t_1, t_2, \ldots, t_{35}$, up to $t_{35} = 40{,}000$ sec. The measurement times are the same for all the MOSFETs.

As depicted in Figure 1, the degradation paths of the units 2–5 are clearly inverse S-shaped. Moreover, the dataset contains 12 negative and 32 null increments, which makes the proposed WP a reasonable candidate for describing these data. Nevertheless, although both the considered transistors and their operating conditions are: nominally identical, the same Figure 1 gives also evidence of the presence of differences among the five paths that can be hardly modeled by a process with independent increments, such as the proposed WP in its basic form. In fact, this type of heterogeneity is usually accounted for by assuming that one or more parameters of the model vary randomly from unit to unit.

On the basis of this guesswork, we have tentatively applied the proposed WP (i.e., the WP (1) with mean function (2)) in the basic form (i.e., by assuming that all the parameters are common to all the units) to the whole set of MOSFET data reported in Table 2. The ML estimates of the model parameters (obtained by maximizing the log-likelihood (24)) are given in Table 2. The corresponding estimated log-likelihood is $\hat{\ell}_0^{(1)} = -40.65$.

Figure 4 shows the ML estimate of the mean function (2) of the process together to the empirical mean evaluated at the measurement epochs. Similarly, Figure 5 displays the ML estimate of the variance function (9) of the process and the empirical estimates of the variance.

As expected, the Figure 5 gives clear evidence that the proposed WP in its basic form is not able to describe adequately the variability exhibited by the MOSFET data, being only able to fit satisfactorily the mean. In fact, the result obtained

TABLE 1 MOSFET degradation data (in percent transconductance loss)

	Unit i						Unit i				
	1	2	3	4	5		1	2	3	4	5
t_j (sec)	$w_{1,j}$	$w_{2,j}$	$w_{3,j}$	$w_{4,j}$	$w_{5,j}$	t_j (sec)	$w_{1,j}$	$w_{2,j}$	$w_{3,j}$	$w_{4,j}$	$w_{5,j}$
100	1.05	0.58	0.86	0.60	0.62	4000	6.60	5.00	4.20	3.00	2.80
200	1.40	0.90	1.25	0.60	0.64	4500	7.00	5.60	4.40	3.00	2.80
300	1.75	1.20	1.45	0.60	1.25	5000	7.80	5.90	4.60	3.00	2.80
400	2.10	1.75	1.75	0.90	1.30	6000	8.60	6.20	4.90	3.60	3.10
500	2.10	2.01	1.75	0.90	0.95	7000	9.10	6.80	5.20	3.60	3.10
600	2.80	2.00	2.00	1.20	1.25	8000	9.50	7.40	5.80	4.20	3.10
700	2.80	2.00	2.00	1.50	1.55	9000	10.50	7.70	6.10	4.60	3.70
800	2.80	2.00	2.00	1.50	1.90	10,000	11.10	8.40	6.30	4.20	4.40
900	3.20	2.30	2.30	1.50	1.25	12,000	12.20	8.90	7.00	4.80	3.70
1000	3.40	2.60	2.30	1.70	1.55	14,000	13.00	9.50	7.20	5.10	4.40
1200	3.80	2.90	2.60	2.10	1.50	16,000	14.00	10.00	7.60	4.80	4.40
1400	4.20	2.90	2.80	2.10	1.55	18,000	15.00	10.40	7.70	5.30	4.10
1600	4.20	3.20	3.15	1.80	1.90	20,000	16.00	10.90	8.10	5.80	4.10
1800	4.50	3.60	3.20	2.10	1.85	25,000	18.50	12.60	8.90	5.70	4.70
2000	4.90	3.80	3.20	2.10	2.20	30,000	20.30	13.20	9.50	6.20	4.70
2500	5.60	4.20	3.80	2.40	2.20	35,000	22.10	15.40	11.20	8.00	6.40
3000	5.90	4.40	3.80	2.70	2.50	40,000	24.20	18.10	14.00	10.90	9.40
3500	6.30	4.80	4.00	2.70	2.20						

TABLE 2 ML estimates of parameters obtained from the whole dataset under the basic model

ML estimates				
$\hat{\alpha}_1$(sec)	$\hat{\beta}_1$	$\hat{\alpha}_2$(sec)	$\hat{\beta}_2$	$\hat{\sigma}_0$
206.7	0.4797	35,166	8.048	0.549

for the variance function is the one that is typically obtained when a model that does not account for the presence of unit-to-unit variability is used to fit a set of heterogeneous degradation paths.

Hence, to verify whether an extended version of the proposed WP that incorporates random effects could adequately fit the considered degradation paths, we have carried out an ad hoc extensive preliminary investigation. The aim of this preliminary study was to identify the parameters to be treated as random into the suggested model, to assign them a (possibly mathematically convenient) probability distribution that properly describes the way in which these parameters vary from unit to unit, and then to check whether the resulting model was actually able to adequately fit the observed data, accounting for all the existing forms of variability.

The preliminary study is illustrated in detail in the Appendix. Obtained results prove that the proposed WP with common parameters β_1, α_2, and β_2, and unit-specific parameters α_1 and σ_0, fits well the MOFETs degradation paths. Thus, in the following, the WP (1) with mean function (2) and random parameters α_1 and σ_0 will be adopted.

4.1 | Degradation process with random effects

The objective of this subsection is incorporating random effects into the proposed WP in order to fully describe all the observed forms of variability. Based on the results of the preliminary analyses illustrated in the Appendix, which proved

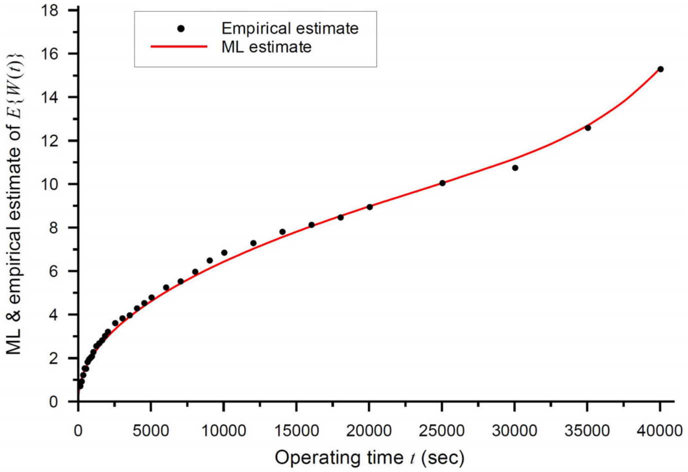

FIGURE 4 ML estimates of the mean function $E\{W(t)\}$ of the basic model (solid line) and empirical estimates of the degradation mean (dots) at the measurement epochs

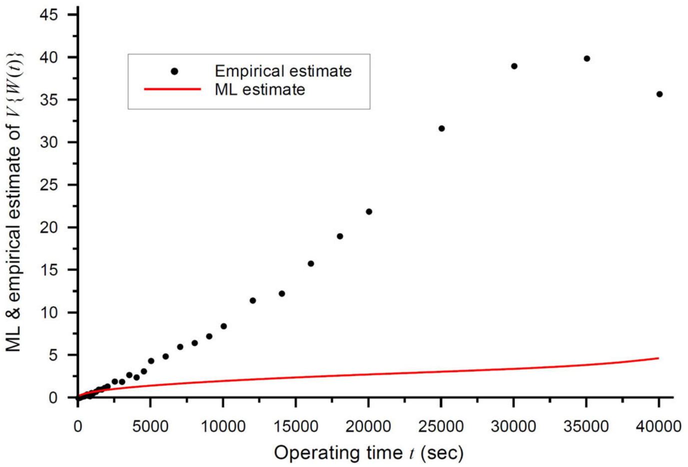

FIGURE 5 ML estimates of the variance function $V\{W(t)\}$ (solid line) of the basic model and empirical estimates of the degradation variance (dots) at the measurement epochs

that the only parameters that can be assumed to be unit-specific are α_1 and σ_0, we will use the proposed WP, with mean function (2), under the assumption that the parameters α_1 and σ_0 are random.

This modeling solution allows to estimate all the parameters of the model taking full (direct) advantage of all the available degradation data and to predict the evolution of the degradation process of a generic transistor that pertains to the considered population, taking into account that some features of its degradation path are unit-specific.

More specifically, we assume that the scale parameter α_1 is distributed as a Gamma random variable with positive shape parameter c and scale parameter d:

$$f(\alpha_1) = \frac{\alpha_1^{c-1}}{d^c\,\Gamma(c)}\,\exp(-\alpha_1/d)\,, \quad \alpha_1 \geq 0, \tag{25}$$

and that the squared diffusion coefficient $\nu = \sigma_0^2$ (i.e., assumed to be stochastically independent on α_1) is distributed as an inverse gamma variable with positive shape parameter a and scale parameter b:

$$f(\nu) = \frac{b^a}{\Gamma(a)}\,\frac{1}{\nu^{a+1}}\exp(-b/\nu), \quad \nu \geq 0\,. \tag{26}$$

TABLE 3 Point ML estimates of the process parameters when α_1 and v are random

ML estimates						
$\hat{c}$	$\hat{d}$ (sec)	$\hat{\beta}_1$	$\hat{\alpha}_2$(sec)	$\hat{\beta}_2$	$\hat{a}$	$\hat{b}$
2.002	124.8	0.4658	35,372	8.346	2.411	0.406

The choice to assign this inverse gamma distribution to v is due to numerical opportunity, because, as shown below, this choice allows to reduce the mathematical complexity of the model. In addition, both the gamma and the inverse gamma distributions are quite flexible to model different behaviors. Under this latter setting, from (23), the conditional likelihood function relative to the generic unit i ($i = 1, \ldots, 5$), given the process parameters α_1 and v, is given by:

$$\mathcal{L}(\boldsymbol{\delta}_i|\alpha_1, v) = \left(\frac{1}{2\pi}\right)^{n/2} \frac{P}{v^{n/2}} \exp\left(-\frac{S_i}{v}\right), \tag{27}$$

where:

$$P = \prod_{j=1}^{n} \left[\Delta\Lambda\left(t_{j-1}, t_j - t_{j-1}\right)\right]^{-1/2},$$
$$S_i = \sum_{j=1}^{n} \frac{1}{2} \frac{\left(\delta_{i,j} - \Delta\Lambda\left(t_{j-1}, t_j - t_{j-1}\right)\right)^2}{\Delta\Lambda\left(t_{j-1}, t_j - t_{j-1}\right)},$$

and $t_0 = 0$. It is worth to note that both P and S_i depend on α_1 through $\Delta\Lambda(\cdot,\cdot)$ (see (2)).

The marginal likelihood $\mathcal{L}(\boldsymbol{\delta}_i)$ relative to the unit i can be expressed as:

$$\begin{aligned}
\mathcal{L}(\boldsymbol{\delta}_i) &= \int_0^\infty \int_0^\infty \mathcal{L}(\boldsymbol{\delta}_i|\alpha_1, v)\, f(\alpha_1)\, f(v)\, \mathrm{d}v\, \mathrm{d}\alpha_1 \\
&= \left(\frac{1}{2\pi}\right)^{n/2} \frac{b^a}{d^c} \frac{1}{\Gamma(a)\,\Gamma(c)} \int_0^\infty P\, \alpha_1^{c-1} \exp\left(-\frac{\alpha_1}{d}\right) \left(\int_0^\infty \frac{\exp\left[-\left(S_i + b\right)/v\right]}{v^{n/2+a+1}} \mathrm{d}v\right) \mathrm{d}\alpha_1 \\
&= \left(\frac{1}{2\pi}\right)^{n/2} \frac{b^a}{d^c} \frac{\Gamma(n/2+a)}{\Gamma(a)\,\Gamma(c)} \int_0^\infty \frac{P\, \alpha_1^{c-1} \exp(-\alpha_1/d)}{\left(S_i + b\right)^{n/2+a}} \mathrm{d}\alpha_1
\end{aligned} \tag{28}$$

The (marginal) likelihood $\mathcal{L}(\boldsymbol{\delta}_i)$ is not in closed form and hence its computation requires a (numerical) univariate integration.

From (28), the log-likelihood function relative to all $m = 5$ units is given by:

$$\ell(\boldsymbol{\theta}|\boldsymbol{\delta}) = \sum_{i=1}^{m} \ln(\mathcal{L}(\boldsymbol{\delta}_i)), \tag{29}$$

where $\boldsymbol{\theta} = (c, d, \beta_1, \alpha_2, \beta_2, a, b)$ is the parameter vector of the process. The maximization of $\ell(\boldsymbol{\theta}|\boldsymbol{\delta})$ requires the numerical computation of $m = 5$ univariate integrals. The point ML estimates of the parameters of the proposed WP with random α_1 and v, are given in Table 3.

From the values in Table 3, we can note that the ML estimates of the fixed parameters β_1, α_2, and β_2, under the assumption that α_1 and v are random, are very close to the ML estimates reported in Table 2 obtained under the assumption that all process parameters values are not unit-specific.

From (2) and (25), the degradation mean of the transistors population is in closed form:

$$E\{W(t)\} = \int_0^\infty (t/\alpha_1)^{\beta_1} f(\alpha_1)\, \mathrm{d}\alpha_1 + (t/\alpha_2)^{\beta_2} = \left(\frac{t}{d}\right)^{\beta_1} \frac{\Gamma(c-\beta_1)}{\Gamma(c)} + \left(\frac{t}{\alpha_2}\right)^{\beta_2}, \tag{30}$$

and its ML estimate is depicted in Figure 6 together to the empirical estimate of the mean at the measurement times. The plot shows a good fit of the proposed model to the observed data.

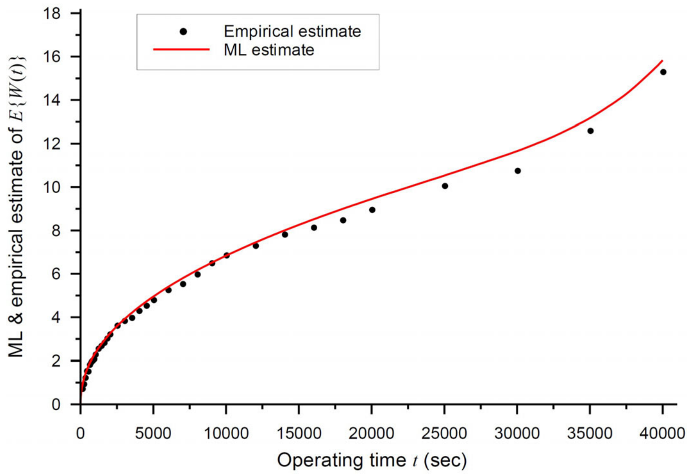

FIGURE 6 ML and empirical estimates of the degradation mean $E\{W(t)\}$

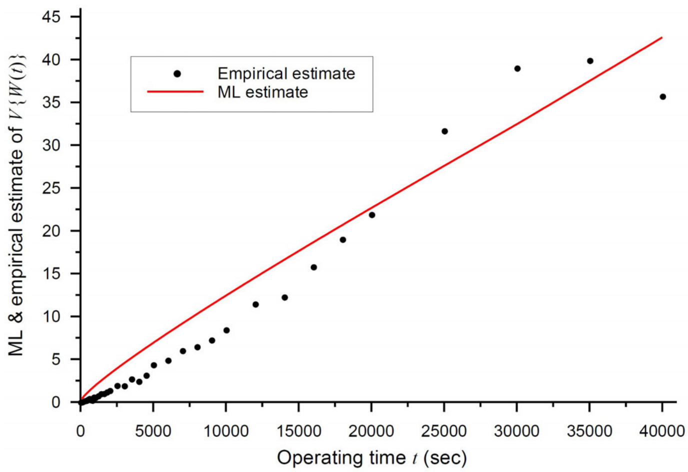

FIGURE 7 ML and empirical estimates of the degradation variance $V\{W(t)\}$

From (9), (25), and (26), the variance function of the process can be expresses as:

$$\begin{aligned}
V\{W(t)\} &= E\left\{[W(t)]^2\right\} - [E\{W(t)\}]^2 \\
&= \int_0^{\infty}\int_0^{\infty}\left\{v\left[\left(\frac{t}{\alpha_1}\right)^{\beta_1}+\left(\frac{t}{\alpha_2}\right)^{\beta_2}\right]+\left[\left(\frac{t}{\alpha_1}\right)^{\beta_1}+\left(\frac{t}{\alpha_2}\right)^{\beta_2}\right]^2\right\} f(\alpha_1)f(v)\,\mathrm{d}\alpha_1\mathrm{d}v - \left[\left(\frac{t}{d}\right)^{\beta_1}\frac{\Gamma(c-\beta_1)}{\Gamma(c)}+\left(\frac{t}{\alpha_2}\right)^{\beta_2}\right]^2 \\
&= \frac{b}{a-1}\left[\left(\frac{t}{d}\right)^{\beta_1}\frac{\Gamma(c-\beta_1)}{\Gamma(c)}+\left(\frac{t}{\alpha_2}\right)^{\beta_2}\right]+\left(\frac{t}{d}\right)^{2\beta_1}\left\{\frac{\Gamma(c-2\beta_1)}{\Gamma(c)}-\left[\frac{\Gamma(c-\beta_1)}{\Gamma(c)}\right]^2\right\}.
\end{aligned}$$

The ML estimate of the variance function is depicted in Figure 7 together to the empirical estimate of variance at the measurements times. This plot shows that the proposed model with random effects describes the empirical variance much better than the basic model (see Figure 5), providing a fit that, although not fully satisfactory, is very good, also taking into account that each empirical estimate is obtained on the basis of only 5 observations.

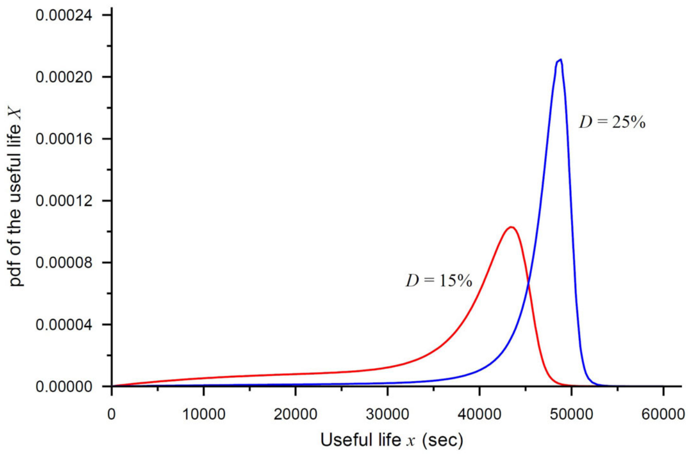

FIGURE 8 ML estimate of the pdf of the useful life X for $D = 15\%$ and $D = 25\%$

From (21), (25), and (26), the pdf of the useful life X of a generic resistor, randomly selected from the considered population, is given by:

$$\begin{aligned} f_X(x) &= \int_0^\infty \int_0^\infty f_X\left(x|\alpha_1, v\right) f\left(\alpha_1\right) f(v)\, \mathrm{d}v \mathrm{d}\alpha_1 \\ &= \frac{D}{\sqrt{2\pi}} \frac{b^a}{d^c\, \Gamma(a)\Gamma(c)} \int_0^\infty \frac{\alpha_1^{c-1} \exp\left(-\frac{\alpha_1}{d}\right)}{[\Lambda(x)]^{\frac{3}{2}}} \frac{\mathrm{d}\Lambda(x)}{\mathrm{d}x} \left(\int_0^\infty \frac{1}{v^{a+\frac{3}{2}}} \exp\left[-\frac{1}{v}\left(\frac{[D-\Lambda(x)]^2}{2\,\Lambda(x)} + b\right)\right] \mathrm{d}v\right) \mathrm{d}\alpha_1 \\ &= \frac{D}{\sqrt{2\pi}} \frac{b^a \Gamma(a+1/2)}{d^c\, \Gamma(a)\, \Gamma(c)} \int_0^\infty \frac{\alpha_1^{c-1}\, \exp(-\alpha_1/d)}{[\Lambda(x)]^{3/2}} \frac{\mathrm{d}\Lambda(x)}{\mathrm{d}x} \left(\frac{[D-\Lambda(x)]^2}{2\,\Lambda(x)} + b\right)^{-a-1/2} \mathrm{d}\alpha_1\,. \end{aligned} \tag{31}$$

Its ML estimate is provided in Figure 8 for $D = 15\%$ and $D = 25\%$.

From (25)–(28), the joint conditional pdf of the parameters α_1 and v, given the vector of increments $\boldsymbol{\delta}_i$ of the unit i, is given by:

$$\begin{aligned} f\left(\alpha_1, v|\boldsymbol{\delta}_i\right) = \frac{\mathcal{L}\left(\boldsymbol{\delta}_i|\alpha_1, v\right) f\left(\alpha_1\right) f(v)}{\mathcal{L}\left(\boldsymbol{\delta}_i\right)} &= \frac{1}{C_\alpha} \frac{\left(\frac{1}{2\pi}\right)^{n/2} \frac{b^a}{d^c} \frac{1}{\Gamma(a)\,\Gamma(c)} \frac{P\, \alpha_1^{c-1}}{v^{n/2+a+1}}}{\left(\frac{1}{2\pi}\right)^{n/2} \frac{b^a}{d^c} \frac{\Gamma(n/2+a)}{\Gamma(a)\,\Gamma(c)}} \exp\left(-\frac{\alpha_1}{d} - \frac{S_i+b}{v}\right) \\ &= \frac{1}{C_\alpha} \frac{1}{\Gamma(n/2+a)} \frac{P\, \alpha_1^{c-1}}{v^{n/2+a+1}} \exp\left(-\frac{\alpha_1}{d} - \frac{S_i+b}{v}\right), \end{aligned} \tag{32}$$

where:

$$C_\alpha = \int_0^\infty \frac{P\, \alpha_1^{c-1}}{\left(S_i+b\right)^{n/2+a}} \exp\left(-\frac{\alpha_1}{d}\right) \mathrm{d}\alpha_1\,. \tag{33}$$

From (32), the marginal conditional pdfs of α_1 and v, given the vector of increments $\boldsymbol{\delta}_i$ of the unit i, easily follow:

$$f\left(\alpha_1|\boldsymbol{\delta}_i\right) = \int_0^\infty f\left(\alpha_1, v|\boldsymbol{\delta}_i\right) \mathrm{d}v = \frac{1}{C_\alpha} \frac{P\, \alpha_1^{c-1}}{\left(S_i+b\right)^{n/2+a}} \exp\left(-\frac{\alpha_1}{d}\right) \tag{34}$$

$$f\left(v|\boldsymbol{\delta}_i\right) = \int_0^\infty f\left(\alpha_1, v|\boldsymbol{\delta}_i\right) \mathrm{d}\alpha_1 = \frac{1}{C_\alpha} \frac{1}{\Gamma(n/2+a)} \frac{1}{v^{n/2+a+1}} \int_0^\infty P\, \alpha_1^{c-1} \exp\left(-\frac{\alpha_1}{d} - \frac{S_i+b}{v}\right) \mathrm{d}\alpha_1. \tag{35}$$

In Figures 9 and 10 the ML estimates of the conditional pdfs $f\left(\alpha_1|\boldsymbol{\delta}_i\right)$ and $f\left(v|\boldsymbol{\delta}_i\right)$ relative to each unit i ($i = 1, \ldots, 5$) are depicted. The randomness of the scale parameter α_1 and of the squared diffusion coefficient $v = \sigma_0^2$ is evident.

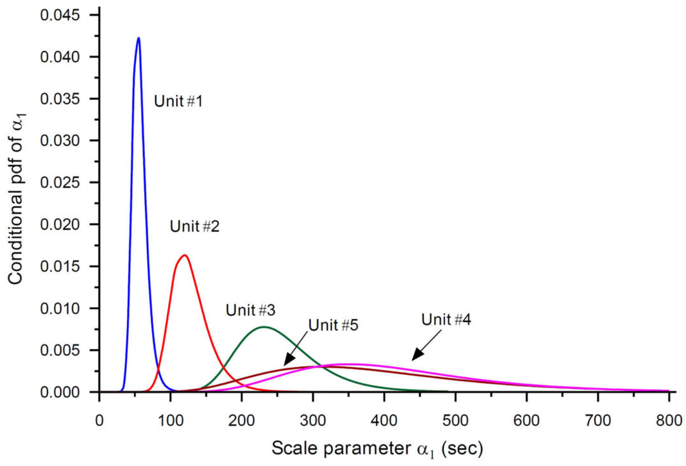

FIGURE 9 ML estimate of the conditional pdf of α_1 of each unit i, given the observed degradation increments of the unit

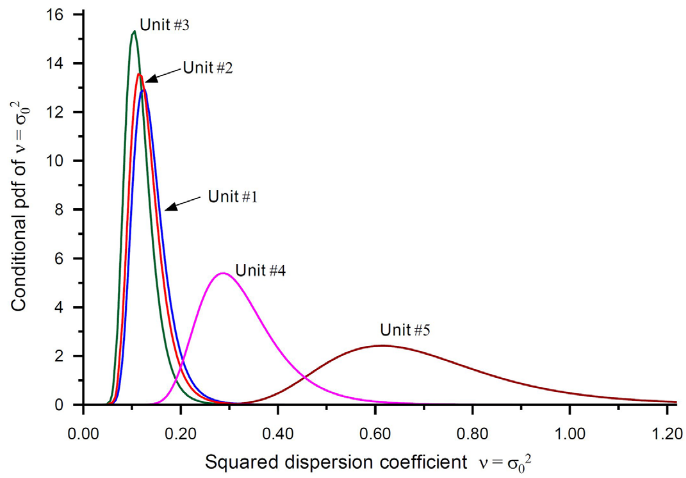

FIGURE 10 ML estimate of the conditional pdf of $\nu = \sigma_0^2$ of each unit i, given the observed degradation increments of the unit

In addition, from the conditional pdf $f\,(\alpha_1|\boldsymbol{\delta}_i)$ in (34), it is easy to obtain the conditional pdf of the inflection point t_{infl} in (5), which does not depend on ν. Indeed, by making the change of variable

$$\alpha_1 = \left[-\alpha_2 \frac{\beta_1\,(\beta_1 - 1)}{\beta_2\,(\beta_2 - 1)}\right]^{1/\beta_1} t_{infl}^{1-\beta_2/\beta_1}, \tag{36}$$

the conditional pdf $f\left(t_{infl}|\boldsymbol{\delta}_i\right)$ of the inflection point, given the vector of increments $\boldsymbol{\delta}_i$ of the unit i, is given by:

$$f\left(t_{infl}|\boldsymbol{\delta}_i\right) = \frac{1}{C_\alpha}\,\frac{P}{(S_i + b)^{n/2+a}}\left[-\alpha_2 \frac{\beta_1\,(\beta_1 - 1)}{\beta_2\,(\beta_2 - 1)}\right]^{(c-1)/\beta_1} t_{infl}^{(c-1)(1-\beta_2/\beta_1)} \exp\left\{-\frac{\left[-\alpha_2 \frac{\beta_1(\beta_1-1)}{\beta_2(\beta_2-1)}\right]^{1/\beta_1} t_{infl}^{1-\beta_2/\beta_1}}{d}\right\}\left|\frac{\mathrm{d}\alpha_1}{\mathrm{d}t_{infl}}\right|, \tag{37}$$

where

$$\left|\frac{\mathrm{d}\alpha_1}{\mathrm{d}t_{infl}}\right| = \left[-\alpha_2 \frac{\beta_1\,(\beta_1 - 1)}{\beta_2\,(\beta_2 - 1)}\right]^{1/\beta_1} t_{infl}^{-\beta_2/\beta_1}\left|1 - \frac{\beta_2}{\beta_1}\right|.$$

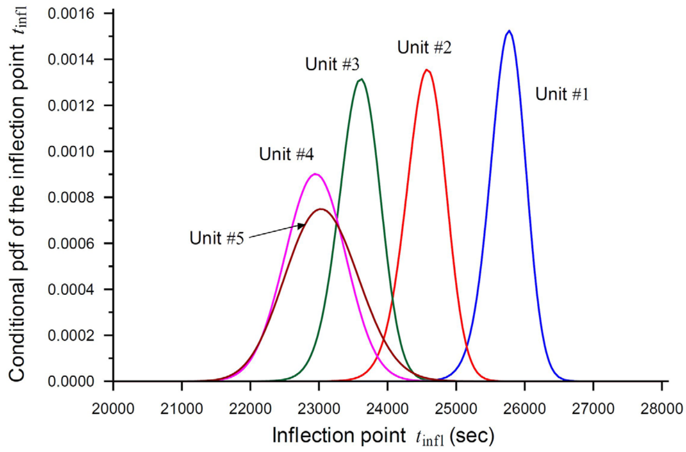

FIGURE 11 ML estimate of the conditional pdf of the inflection point t_{infl} of each unit i, given the observed degradation increments of the unit

In Figure 11 the ML estimates of the conditional pdf $f\left(t_{infl}|\boldsymbol{\delta}_i\right)$ relative to each unit i ($i = 1, \ldots, 5$) are depicted. The randomness of the inflection point over the five units is evident.

From (7), the conditional pdf of the degradation increment $\Delta W(t_n, \tau)$ during the (future) time interval $(t_n, t_n + \tau)$, given α_1 and $v = \sigma_0^2$, is given by:

$$f_{\Delta W(t_n,\tau)}(\delta|\alpha_1, v) = \frac{1}{\sqrt{2\pi\, v\, \Delta\Lambda(t_n,\tau)}} \exp\left[-\frac{1}{2}\left(\frac{(\delta - \Delta\Lambda(t_n,\tau))^2}{v\,\Delta\Lambda(t_n,\tau)}\right)\right], \tag{38}$$

where $\Delta\Lambda(t_n, \tau)$ depends, of course, on α_1. From (32) and (38), the conditional pdf of the (future) degradation increment $\Delta W(t_n, \tau)$ of the unit i, given the vector of the observed increments $\boldsymbol{\delta}_i$ until $t_n = 40{,}000$ sec, is given by:

$$\begin{aligned} f_{\Delta W(t_n,\tau)}(\delta|\boldsymbol{\delta}_i) &= \int_0^\infty \int_0^\infty f_{\Delta W(t_n,\tau)}(\delta|\alpha_1, v)\, f(\alpha_1, v|\boldsymbol{\delta}_i)\, \mathrm{d}v\, \mathrm{d}\alpha_1 \\ &= \frac{1}{C_\alpha}\frac{1}{\sqrt{2\pi}}\frac{1}{\Gamma(n/2+a)}\int_0^\infty \frac{P\,\alpha_1^{c-1}\exp(-\alpha_1/d)}{\sqrt{\Delta\Lambda(t_n,\tau)}}\left(\int_0^\infty \frac{\exp\left[-\frac{1}{v}\left(\frac{(\delta-\Delta\Lambda(t_n,\tau))^2}{2\,\Delta\Lambda(t_n,\tau)} + S_i + b\right)\right]}{v^{n/2+a+3/2}}\mathrm{d}v\right)\mathrm{d}\alpha_1 \\ &= \frac{1}{C_\alpha}\frac{1}{\sqrt{2\pi}}\frac{\Gamma(n/2+a+1/2)}{\Gamma(n/2+a)}\int_0^\infty \frac{P\,\alpha_1^{c-1}\exp(-\alpha_1/d)}{\frac{(\delta-\Delta\Lambda(t_n,\tau))^2}{2\,\Delta\Lambda(t_n,\tau)} + S_i + b}\frac{1}{\sqrt{\Delta\Lambda(t_n,\tau)}}\mathrm{d}\alpha_1. \end{aligned} \tag{39}$$

The conditional Cdf and the conditional mean of the degradation increment, given $\boldsymbol{\delta}_i$, are respectively:

$$F_{\Delta W(t_n,\tau)}(\delta|\boldsymbol{\delta}_i) = \int_0^\delta f_{\Delta W(t_n,\tau)}(z|\boldsymbol{\delta}_i)\,\mathrm{d}z \tag{40}$$

$$E\{\Delta W(t_n\tau)|\boldsymbol{\delta}_i\} = \int_0^\infty \delta\, f_{\Delta W(t_n,\tau)}(z|\boldsymbol{\delta}_i)\,\mathrm{d}z. \tag{41}$$

In Figure 12 the ML estimate of the conditional pdfs of the degradation increment $\Delta W(t_n, \tau)$ of the unit i ($i = 1, \ldots, 5$) for $\tau = 10{,}000$ sec are depicted. All the above pdfs are centered roughly around the same mean value (the estimated mean of the degradation increment ranges indeed from 15.9 to 17.6), due to the limited influence of the (random) scale parameter α_1 on the distribution of the future degradation increment, whereas the noticeable differences in the variance of the above pdfs is due to the random nature of the squared diffusion coefficient $\upsilon = \sigma_0^2$.

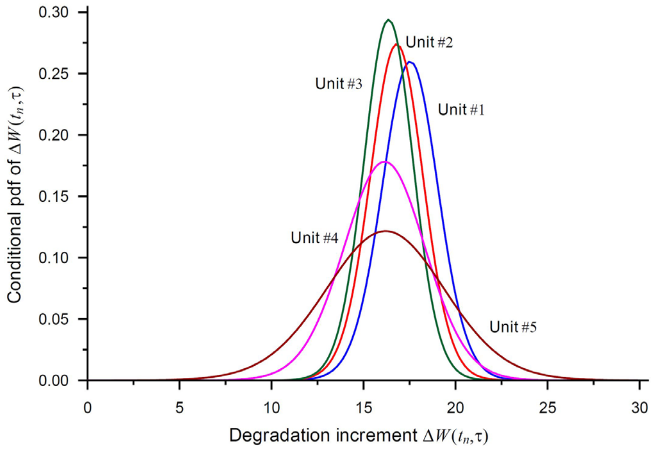

FIGURE 12 ML estimate of the conditional pdf of the increment $\Delta W(t_n, \tau)$ of each unit i, for $\tau = 10{,}000$ sec

From (17), the conditional pdf of the remaining useful life (RUL) X_t, given the process parameters α_1 and ν and the degradation level w_t at the current time t, is given by:

$$f_{X_t}(x|\alpha_1, \nu, w_t) = \frac{D - w_t}{\sqrt{2\pi\,\nu}\,[\Delta\Lambda(t_n, x)]^{\frac{3}{2}}} \exp\left[-\frac{1}{2}\,\frac{(D - w_t - \Delta\Lambda(t_n, x))^2}{\nu\,\Delta\Lambda(t_n, x)}\right] \frac{\mathrm{d}\Delta\Lambda(t_n, x)}{\mathrm{d}x}, \tag{42}$$

whereas, form (18), the conditional Cdf is given by:

$$F_{X_t}(x|\alpha_1, \nu, w_t) = \Phi\left(\sqrt{\frac{\lambda}{\Lambda(t_n, x)}}\left(\frac{\Delta\Lambda(t_n, x)}{D - w_t} - 1\right)\right) \exp\left[\frac{2(D - w_t)}{\nu}\right] \Phi\left(-\sqrt{\frac{\lambda}{\Delta\Lambda(t_n, x)}}\left(\frac{\Delta\Lambda(t_n, x)}{D - w_t} + 1\right)\right), \tag{43}$$

where $\lambda = (D - w_t)^2/\nu$. Thus, the conditional pdf of the RUL of the unit i at time t_n, which for economy of notation is indicated as X_n, given the vector of the observed increments $\boldsymbol{\delta}_i$ until t_n, is given by:

$$\begin{aligned} f_{X_n}(x|\boldsymbol{\delta}_i) &= \int_0^\infty \int_0^\infty f_{X_n}\left(x|\alpha_1, \nu, w_{i,n}\right) f(\alpha_1, \nu|\boldsymbol{\delta}_i)\,\mathrm{d}\nu\mathrm{d}\alpha_1 \\ &= \frac{D - w_{i,n}}{C_\alpha\,\sqrt{2\pi}}\,\frac{1}{\Gamma(n/2 + a)} \int_0^\infty \frac{P\,\alpha_1^{c-1}\exp(-\alpha_1/d)}{[\Delta\Lambda(t_n, x)]^{3/2}}\,\frac{\mathrm{d}\Delta\Lambda(t_n, x)}{\mathrm{d}x} \\ &\quad\times\left(\int_0^\infty \frac{1}{\nu^{n/2+a+3/2}}\,\exp\left[-\frac{1}{\nu}\left(\frac{\left(w_{\mathrm{M}} - w_{i,n} - \Delta\Lambda(t_n, x)\right)^2}{2\,\Delta\Lambda(t_n, x)} + S_i + b\right)\right]\mathrm{d}\nu\right)\mathrm{d}\alpha_1 \\ &= \frac{1}{C_\alpha}\,\frac{D - w_{i,n}}{\sqrt{2\pi}}\,\frac{\Gamma(n/2 + a + 1/2)}{\Gamma(n/2 + a)} \int_0^\infty \frac{P\,\alpha_1^{c-1}\exp(-\alpha_1/d)}{\left[\frac{(D - w_{i,n} - \Delta\Lambda(t_n, x))^2}{2\,\Delta\Lambda(t_n, x)} + S_i + b\right]^{n/2+a+1/2}}\,\frac{1}{[\Delta\Lambda(t_n, x)]^{3/2}}\,\frac{\mathrm{d}\Delta\Lambda(t_n, x)}{\mathrm{d}x}\,\mathrm{d}\alpha_1, \end{aligned} \tag{44}$$

where $w_{i,n} = \sum_{j=1}^{n} \delta_{i,j}$ is the degradation level of the unit i measured at the last observation time t_n, and from (19):

$$\frac{\mathrm{d}\Delta\Lambda(t_n, x)}{\mathrm{d}x} = \frac{\beta_1}{\alpha_1}\left(\frac{t_n + x}{\alpha_1}\right)^{\beta_1 - 1} + \frac{\beta_2}{\alpha_2}\left(\frac{t_n + x}{\alpha_2}\right)^{\beta_2 - 1}. \tag{45}$$

The (conditional) residual reliability of the unit i and the conditional mean of its RUL X_n, given $\boldsymbol{\delta}_i$, are:

$$R_{X_n}(x|\boldsymbol{\delta}_i) = 1 - \int_0^x f_{X_n}(z|\boldsymbol{\delta}_i)\,\mathrm{d}z \tag{46}$$

$$E\{X_n|\boldsymbol{\delta}_i\} = \int_0^\infty x\,f_{X_n}(x|\boldsymbol{\delta}_i)\,\mathrm{d}x, \tag{47}$$

respectively.

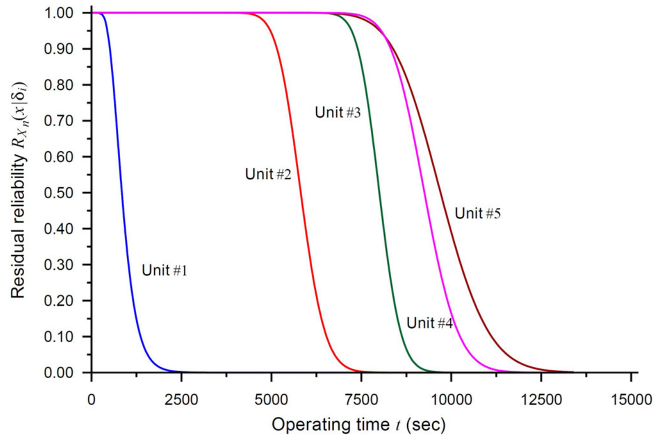

FIGURE 13 ML estimate of the residual reliability of each unit i, for $D = 25\%$

TABLE 4 ML estimate of the conditional mean of the remaining useful life (in sec), for $D = 25\%$

Unit	1	2	3	4	5
$\hat{E}\{X_n|\boldsymbol{\delta}_i\}$	901	5834	8010	9270	9732

In Figure 13, the ML estimate of the residual reliability function (46) of the unit i ($i = 1, \ldots, 5$), given all observed increments of the unit, is depicted, having assumed that the failure threshold is $D = 25\%$. The estimates of the conditional mean (47) of the RUL (in sec) are given in Table 4.

An important feature of the proposed WP is that it allows to make inference, for example, on the RUL and on the (random) inflection point of a new unit belonging to the considered heterogeneous population also from data collected only during the early phase of its useful life. Thus, let $t_j^{(N)}$ and $\delta_j^{(N)}$ ($j = 1, \ldots, k$) denote, respectively, the k inspection times and the observed degradation increments of the new unit over the time intervals $\left(t_{j-1}^{(N)}, t_j^{(N)}\right)$, with $t_0^{(N)} = 0$.

In particular, under the assumed WP with random α_1 and σ_0, from (44), the conditional pdf of the RUL $X_k^{(N)}$ of the new unit, evaluated at time $t_k^{(N)}$, given the vector $\boldsymbol{\delta}_k^{(N)} = \left(\delta_1^{(N)}, \ldots, \delta_k^{(N)}\right)$ of the observed "early" increments, is given by:

$$f_{X_k^{(N)}}\left(x|\boldsymbol{\delta}_k^{(N)}\right) = \frac{1}{C_\alpha^{(N)}}\frac{D - w_k^{(N)}}{\sqrt{2\pi}}\frac{\Gamma(k/2 + a + 1/2)}{\Gamma(k/2 + a)}$$
$$\times \int_0^\infty \frac{P^{(N)}\,\alpha_1^{c-1}\exp(-\alpha_1/d)}{\left[\frac{\left(D - w_k^{(N)} - \Delta\Lambda\left(t_k^{(N)}, x\right)\right)^2}{2\,\Lambda\left(t_k^{(N)}, x\right)} + S^{(N)} + b\right]^{k/2+a+1/2}} \frac{1}{\left[\Delta\Lambda\left(t_k^{(N)}, x\right)\right]^{3/2}} \frac{\mathrm{d}\Delta\Lambda\left(t_k^{(N)}, x\right)}{\mathrm{d}x}\,\mathrm{d}\alpha_1, \tag{48}$$

where $w_k^{(N)} = \sum_{j=1}^{k}\delta_j^{(N)}$ is the degradation level at the last early observation time of the new unit:

$$P^{(N)} = \prod_{j=1}^{k}\left[\Lambda\left(t_{j-1}^{(N)}, t_j^{(N)} - t_{j-1}^{(N)}\right)\right]^{-1/2},$$

$$S^{(N)} = \sum_{j=1}^{k}\frac{1}{2}\frac{\left(\delta_j^{(N)} - \Delta\Lambda\left(t_{j-1}^{(N)}, t_j^{(N)} - t_{j-1}^{(N)}\right)\right)^2}{\Delta\Lambda\left(t_{j-1}^{(N)}, t_j^{(N)} - t_{j-1}^{(N)}\right)},$$

$$\frac{\mathrm{d}\Lambda\left(t_k^{(N)}, x\right)}{\mathrm{d}x} = \frac{\beta_1}{\alpha_1}\left(\frac{t_k^{(N)} + x}{\alpha_1}\right)^{\beta_1 - 1} + \frac{\beta_2}{\alpha_2}\left(\frac{t_k^{(N)} + x}{\alpha_2}\right)^{\beta_2 - 1},$$

TABLE 5 The pseudo-random sample $w_j^{(N)}, j = 1, \ldots, 35$, of a new unit

$t_j^{(N)}$ (sec)	100	200	300	400	500	600	700	800	900
$w_j^{(N)}$	0.66	0.80	1.18	1.47	1.59	1.81	1.97	2.20	2.22
$t_j^{(N)}$ (sec)	1000	1200	1400	1600	1800	2000	2500	3000	3500
$w_j^{(N)}$	2.36	2.67	2.94	3.16	3.34	3.54	3.91	4.44	4.68
$t_j^{(N)}$ (sec)	4000	4500	5000	6000	7000	8000	9000	10,000	12,000
$w_j^{(N)}$	4.98	5.22	5.65	6.16	6.91	7.69	8.04	8.45	9.57
$t_j^{(N)}$ (sec)	14,000	16,000	18,000	20,000	25,000	30,000	35,000	40,000	
$w_j^{(N)}$	10.57	10.89	11.68	12.08	13.58	15.34	17.06	19.25	

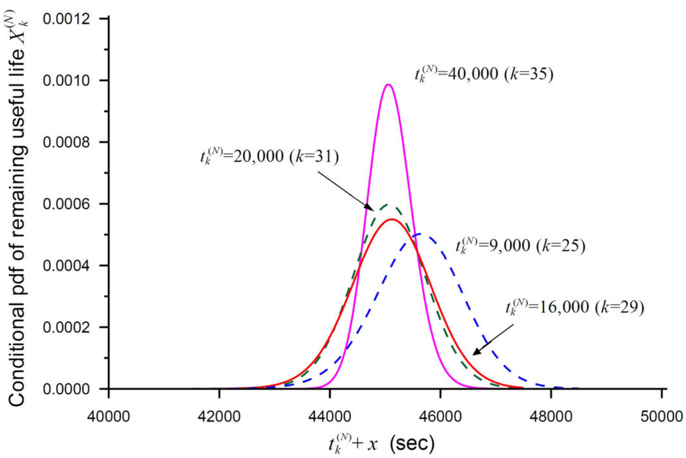

FIGURE 14 Conditional pdfs $f_{X_k^{(N)}}\left(x|\boldsymbol{\delta}_k^{(N)}\right)$ of the RUL of the new unit, given the pseudo-random data $\boldsymbol{\delta}_k^{(N)}$ observed up to $t_k^{(N)} = 9{,}000$, 16,000, 20,000, and 40,000 sec

and

$$C_\alpha^{(N)} = \int_0^\infty \frac{P^{(N)}\ \alpha_1^{c-1}}{\left(S^{(N)} + b\right)^{K/2+a}} \exp\left(-\frac{\alpha_1}{d}\right)\, \mathrm{d}\alpha_1.$$

Of course, the residual reliability $R_{X_k^{(N)}}\left(x|\boldsymbol{\delta}_k^{(N)}\right)$ of the new unit and the conditional mean $E\left\{X_k^{(N)}|\boldsymbol{\delta}_k^{(N)}\right\}$ of its RUL, given the early k data of the new unit, can be easily obtained by numerical integrations, as in (46) and (47).

Likewise, the conditional pdf $f\left(t_{infl}|\boldsymbol{\delta}_k^{(N)}\right)$ of the inflection point t_{infl} of the new unit, given the vector $\boldsymbol{\delta}_k^{(N)} = \left(\delta_1^{(N)}, \ldots, \delta_k^{(N)}\right)$ of the observed "early" increments, can be obtained from (37) by substituting P, S_i, and n with $P^{(N)}$, $S^{(N)}$, and k, respectively.

In order to shows the ability of the proposed WP to make inference on a new unit on the base of its early data, a pseudo-random set of degradation levels measured at the same inspection times t_j ($j = 1, \ldots, 35$) of Table 1 has been simulated by setting the model parameters equal to the ML estimates $\widehat{\beta}_1 = 0.4658$, $\widehat{\alpha}_2 = 35{,}372$ sec, $\widehat{\beta}_2 = 8.346$, and by drawing the unit-specific (pseudo-random) values of α_1 and $v = \sigma_0^2$ from the corresponding estimated distributions (25) and (26), say $\alpha_1 = 98.3$ sec and $v = 0.1204$. This pseudo-random sample is given in Table 5.

Thus, on the basis of the early data gathered up to $t_k^{(N)} = 9000$, 16,000, and 20,000 sec (corresponding to $k = 25$, 29, and 31, respectively), as well as on the basis of the entire pseudo-random sample ($k = 35$), the conditional pdfs of the RUL $X_k^{(N)}$ and of the inflection point t_{infl} of the new unit, given the observed "early" k increments $\boldsymbol{\delta}_k^{(N)}$, have been estimated.

In Figure 14 the conditional pdfs $f_{X_k^{(N)}}\left(x|\boldsymbol{\delta}_k^{(N)}\right)$ are depicted for selected K values, where on the abscissa axis the sum $t_k^{(N)} + x$ is given in order to easily compare the above pdfs.

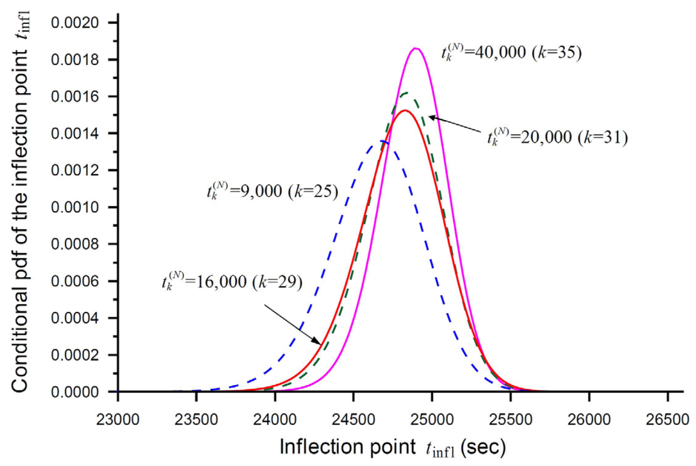

FIGURE 15 Conditional pdfs $f\left(t_{infl}|\delta_k^{(N)}\right)$ of the inflection point of the new unit, given the pseudo-random data $\delta_k^{(N)}$ observed up to $t_k^{(N)} = 9{,}000$, 16,000, 20,000, and 40,000 sec

From Figure 14 we can note that a good estimate of the RUL of the new unit has been obtained also on the basis of its very early data, say those observed up to 9000 sec. In particular, the sum $t_k^{(N)} + E\left\{X_k^{(N)}|\delta_k^{(N)}\right\}$ of last observation time $t_k^{(N)}$ and of the conditional mean $E\left\{X_k^{(N)}|\delta_k^{(N)}\right\}$ of the RUL is equal to 45,092 sec when the entire dataset ($k = 35$) is used, and is equal to 45,601 and 45,102 sec when only the early data observed up to $t_k^{(N)} = 9{,}000$ and 16,000 sec, respectively, are used.

Finally, Figure 15 provides the conditional pdfs $f\left(t_{infl}|\delta_k^{(N)}\right)$ of the inflection point t_{infl} of the new unit for the same selected k values. From this figure, we can note that a good estimate of the inflection point of the new unit has been obtained also on the basis of its early data. In particular, the mean inflection point $E\left\{t_{infl}|\delta^{(N)}\right\}$, obtained by numerical integration of the conditional pdf, is equal to 24,878 sec when the entire dataset ($k = 35$) is used, and is equal to 24,642 and 24,799 sec when the early data observed up to $t_k^{(N)} = 9000$ and 16,000 sec, respectively, are used.

5 | CONCLUSIONS

Although in the literature it is recognized that the degradation rate function (here intended as the derivative of the mean degradation function) of technological units is typically bathtub-shaped, presenting three phases during which the degradation rate decreases, is constant, and decreases, respectively, almost all the Wiener degradation models proposed in the literature are characterized by a monotonic degradation rate function. This circumstance represents a potential limitation for their successfully application in real settings. In fact, models with monotonic degradation rate function are clearly able to describe only two of the mentioned three phases of the degradation phenomena.

Motivated by these arguments and by a set of real degradation data of metal-oxide-semiconductor field-effect transistors (MOSFETs), which exhibit an inverse S-shaped behavior of the (empirical) mean function and (consequently) a bathtub shaped degradation rate function, in this paper we have proposed a new Wiener process that can describe phenomena characterized by bathtub-shaped degradation rate functions.

The main features of the proposed Wiener process, which is formulated under two different parameterizations, have been illustrated and discussed. The remaining useful life (RUL) of a unit and its residual reliability have been formulated by adopting a failure threshold model. Maximum likelihood estimation of the process parameters and some functions thereof has been addressed.

The proposed Wiener process has been then applied to the MOSFET data. Having verified, as a result of preliminary analyses, that the proposed model in its basic form (i.e., in absence of random effects) is not able to adequately fit the MOSFET data, an extended version of the Wiener process, where selected parameters are assumed to vary randomly from unit to unit, has been formulated and applied to the MOSFET data. The obtained results demonstrated the effectiveness and affordability of the proposed approach. In particular, the application gives clear evidence that the proposed process can be successfully used to make inference on the RUL and on the inflection point of a new unit belonging to the considered heterogeneous population also on the basis of its early data alone.

Finally, the formulation of different inverse S-shaped mean degradation functions, able to extend the range of applicability of the proposed Wiener process, will be the subject of future studies and applications.

ACKNOWLEDGMENT

The authors would like to thank the Associate Editor and the anonymous reviewers for their valuable comments and suggestions that allowed to improve the quality of the paper. Open Access Funding provided by Universita degli Studi di Napoli Federico II within the CRUI-CARE Agreement.

DATA AVAILABILITY STATEMENT

The data that supports the findings of this study are available within the article.

ORCID

Massimiliano Giorgio https://orcid.org/0000-0002-5348-5289
Gianpaolo Pulcini https://orcid.org/0000-0001-5474-7095

REFERENCES

1. Abdel-Hameed MA. A gamma wear process. *IEEE Trans Reliab*. 1975;24(2):152-154. doi:10.1109/TR.1975.5215123
2. van Noortwijk JM. A survey of the application of gamma processes in maintenance. *Reliab Eng Syst Saf*. 2009;94(1):2-21. doi:10.1016/j.ress.2007.03.019
3. Ye ZS, Chen N. The inverse Gaussian process as a degradation model. *Technometrics*. 2014;56(3):302-311. doi:10.1080/00401706.2013.830074
4. Whitmore GA, Schenkelberg F. Modelling accelerated degradation data using wiener diffusion with a time scale transformation. *Lifetime Data Anal*. 1997;3(1):27-45. doi:10.1023/A:1009664101413
5. Wang X. Wiener processes with random effects for degradation data. *J Multivar Anal*. 2010;101(2):340-351. doi:10.1016/j.jmva.2008.12.007
6. Wang X, Xu D. An inverse Gaussian process model for degradation data. *Technomtrics*. 2010;52(2):188-197. doi:10.1198/TECH.2009.08197
7. Ye ZS, Chen N, Shen Y. A new class of wiener process models for degradation analysis. *Reliab Eng Syst Saf*. 2015;139:58-67. doi:10.1016/j.ress.2015.02.005
8. Kahle W, Mercier S, Paroissin C. *Degradation Processes in Reliability*. ISTE Ltd and John Wiley & Sons Inc; 2016.
9. Gertsbakh IB, Kordonskiy KB. *Models of Failure*. Springer-Verlag; 1969.
10. Peng W, Li YF, Yang YJ, Mi J, Huang HZ. Bayesian degradation analysis with inverse Gaussian process models under time-varying degradation rates. *IEEE Trans Reliab*. 2017;66(1):84-96. doi:10.1109/TR.2016.2635149
11. Chen Z, Li Y, Zhou D, Xia T, Pan E. Two-phase degradation data analysis with change-point detection based on Gaussian process degradation model. *Reliab Eng Syst Saf*. 2021;216:107916. doi:10.1016/j.ress.2021.107916
12. Wang X, Jiang P, Guo B, Cheng Z. Real-time reliability evaluation for an individual product based on change point gamma and wiener process. *Qual Reliab Eng Int*. 2014;30(4):513-525. doi:10.1002/qre.1504
13. Kong D, Balakrishnan N, Cui L. Two-phase degradation process model with abrupt jump at change point governed by wiener process. *IEEE Trans Reliab*. 2017;66(4):1345-1360. doi:10.1109/TR.2017.2711621
14. Liu K, Zou TJ, Xin MC, Lv CM. RUL prediction based on two-phase wiener process. *Qual Reliab Eng Int*. 2022;38:3829-3843. doi:10.1002/qre.3177
15. Gao H, Cui L, Dong Q. Reliability modeling for a two-phase degradation system with a change point based on a wiener process. *Reliab Eng Syst Saf*. 2020;193:106601. doi:10.1016/j.ress.2019.106601
16. Lin J, Liao G, Chen M, Yin H. Two-phase degradation modeling and remaining useful life prediction using nonlinear wiener process. *Comput Ind Eng*. 2021;160:107533. doi:10.1016/j.cie.2021.107533
17. Xie M, Lai CD. Reliability analysis using an additive Weibull model with bathtub-shaped failure rate function. *Reliab Eng Syst Saf*. 1995;52:87-93. doi:10.1016/0951-8320(95)00149-2
18. Lai CD, Xie M, Murthy DNP. Ch. 3. Bathtub-shaped failure rate life distributions. In: Balakrishnan N, Rao CR, eds. *Handbook of Statistics 20. Elsevier*; 2001:269-104. doi:10.1016/S0169-7161(01)20005-4
19. Nadarajah S. Bathtub-shaped failure rate functions. *Qual Quant*. 2009;43:855-863. doi:10.1007/s11135-007-9152-9
20. Giorgio M, Pulcini G. A new age- and state-dependent degradation process with possibly negative increments. *Qual Reliab Eng*. 2019;35:1476-1501. doi:10.1002/qre.2525
21. Lu JC, Park J, Yang Q. Statistical inference of a time-to-failure distribution derived from linear degradation data. *Technometrics*. 1997;39(4):391-400. doi:10.1080/00401706.1997.10485158

22. Yang G. *Life Cycle Reliability Engineering*. John Wiley & Sons; 2007.
23. Akaike H. A new look at the statistical model identification. *IEEE Trans Automat Contr*. 1974;19(6):716-723. doi:10.1109/TAC.1974.1100705

How to cite this article: Giorgio M, Piscopo A, Pulcini G. A new Wiener process with bathtub-shaped degradation rate in the presence of random effects. *Appl Stochastic Models Bus Ind*. 2023;1-24. doi:10.1002/asmb.2749

APPENDIX A. PRELIMINARY STUDY

The aim of the preliminary study illustrated in this Appendix is to verify whether the proposed WP can adequately fit the individual paths, as well as to verify whether some parameters can be assumed to be common to all the units and which parameters must instead be assumed to be random.

As first step, we have estimated unit-by-unit (i.e., for $i = 1, 2, \dots, 5$) the parameters of the proposed WP (1) with mean function (2), by maximizing the log-likelihood (23). Obtained results are reported in Table A1, together to the coefficient of variation (CV) computed from the estimates of each parameter. The corresponding estimate of the log-likelihood is $\hat{\ell}_1^{(1)} = 4.34$.

Figure A1 shows the observed degradation paths together to the ML estimates of the mean degradation function $E\{W(t)\}$ obtained by computing (unit-by-unit) the mean function (2) at the ML estimates reported in Table A1. The plot gives evidence that the estimated models fit well the observed degradation paths.

For the sake of comparison, we have also modeled the single paths by using the Wiener process with the 3-parameter S-shaped mean function:

$$\Lambda(t) = \varphi\ \exp(\gamma\ t/\varphi - \omega\ \varphi/t), \quad \gamma, \varphi, \omega > 0, \tag{A.1}$$

suggested by Peng et al.[10]

The plots of the ML estimate of the mean functions depicted in Figure A2 give clear evidence that this latter model is not able to fit the MOSFET data.

A formal comparison between the fitting ability of the WP with mean (2) and the WP with mean (A.1) can be performed by using the Akaike information criterion (AIC),[23] which leads to prefer the model with the smaller value of the AIC index. The AIC index is defined as $\text{AIC} = 2k - 2\hat{\ell}$, where k is the number of unknown parameters of the model and $\hat{\ell}$ is the estimated log-likelihood function. On the basis of the estimated log-likelihoods, the AIC value relative to the WP with mean function (2) is equal to 41.31, whereas the AIC value relative to the WP with mean function (A.1) is equal to 137.26, a result that proves the clear superiority of the proposed model in describing the MOSFET data.

So stated, to formally check that the proposed WP with parameters that are all unit-specific fits the MOSFET data better than the proposed WP with all common parameters, we have performed a likelihood ratio test for checking the following null and alternative hypotheses:

TABLE A1 ML estimates of the process parameters and their coefficient of variation under the hypothesis that all parameters are unit-specific

	Unit i					
	1	**2**	**3**	**4**	**5**	***CV***
$\hat{\alpha}_1$ (sec)	95.2	139.2	105.8	566.1	212.5	0.88
$\hat{\beta}_1$	0.5240	0.4804	0.3978	0.4709	0.3455	0.16
$\hat{\alpha}_2$ (sec)	41,439	34,619	34,706	35,016	35,916	0.08
$\hat{\beta}_2$	20.812	7.438	8.624	9.358	11.066	0.47
$\hat{\sigma}_0$	0.310	0.331	0.298	0.597	0.961	0.57

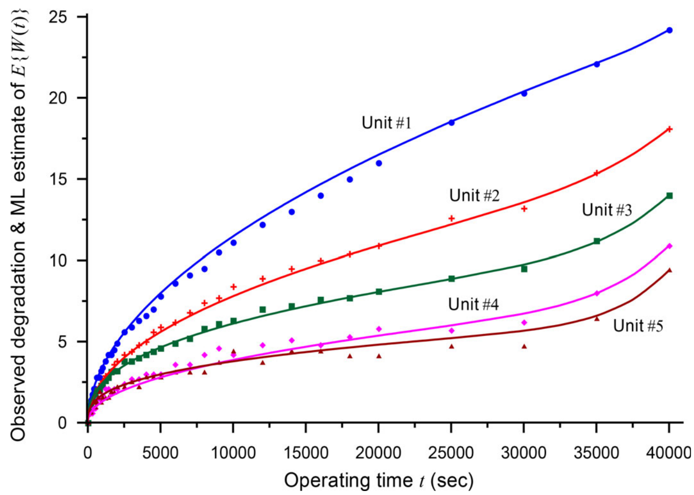

FIGURE A1 Observed degradation data (dots) and ML estimate of $E\{W(t)\}$ of each unit (dashed lines) obtained under the assumption that all the parameters are unit-specific

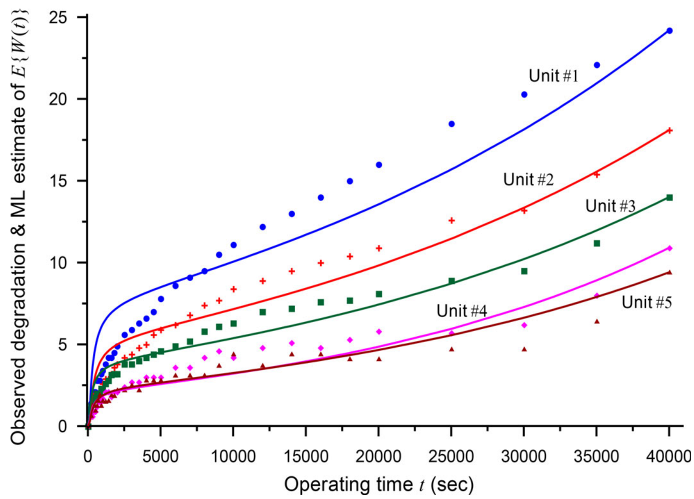

FIGURE A2 Observed degradation data (dots) and ML estimate of $E\{W(t)\}$ of each unit (dashed lines) obtained by using the WP with mean function (A.1), under the assumption that all the parameters are unit-specific

- null hypothesis $H_0^{(1)}$: all parameters are common;
- alternative hypothesis $H_1^{(1)}$: all parameters are unit-specific.

The corresponding test statistic $\Lambda^{(1,1)} = -2 \cdot \left(\hat{\ell}_0^{(1)} - \hat{\ell}_1^{(1)}\right)$ takes the value $-2 \cdot (-40.65 - 4.34) = 90.00$. Under the null hypothesis $H_0^{(1)}$ the test statistic $\Lambda^{(1,1)}$ is approximately distributed as a chi-square random variable with $25 - 5 = 20$ degrees of freedom (dof). The resulting p-value is $p^{(1,1)} = 7 \cdot 10^{-11}$, thus confirming that the null hypothesis $H_0^{(1)}$ should be rejected at any plausible significance level.

The value of the coefficients of variation (CV) of each parameter given in the last column of Table A1 depends on two contributions: (i) the fluctuation of estimates due to random sampling, and (ii) the (possible) existence of heterogeneity among the values of the parameter used to describe the degradation path of different units. Hence, it is realistic to expect that the parameters that are unit-specific are those with the highest CV. Based on this semi-heuristic rule, we begin our investigation by supposing that only α_1, β_2, and σ_0 are unit-specific. Hence, in order to check whether this latter WP provides a better trade-off between complexity and fitting ability than the WP where all the parameters are unit-specific, the likelihood ratio test is again applied to check the following null and alternative hypotheses:

TABLE A2 Likelihood ratio test results relative to MOSFET data, under the original parameterization

Null hypothesis H_0	Alternative hypothesis H_1	Λ	dof	p-value	Decision
All parameters are common	All parameters are unit-specific	90.00	20	$7 \cdot 10^{-11}$	Reject H_0
Only α_1, β_2, and σ_0 are unit-specific	All parameters are unit-specific	5.25	8	0.731	Not reject H_0
Only α_1 and β_2 are unit-specific	α_1, β_2, and σ_0 are unit-specific	51.18	4	$2 \cdot 10^{-10}$	Reject H_0
Only α_1 and σ_0 are unit-specific	α_1, β_2, and σ_0 are unit-specific	6.60	4	0.159	Not reject H_0
Only β_2 and σ_0 are unit-specific	α_1, β_2, and σ_0 are unit-specific	46.50	4	$2 \cdot 10^{-9}$	Reject H_0
Only α_1 is unit-specific	α_1 and σ_0 are unit-specific	47.79	4	$2 \cdot 10^{-8}$	Reject H_0
Only σ_0 is unit-specific	α_1 and σ_0 are unit-specific	41.84	4	$1 \cdot 10^{-9}$	Reject H_0

- null hypothesis $H_0^{(2)}$: only α_1, β_2, and σ_0 are unit-specific,
- alternative hypothesis $H_1^{(1)}$: all parameters are unit-specific.

The parameters under the null hypothesis $H_0^{(2)}$ have been therefore estimated, and the resulting estimated log-likelihood is equal to $\hat{\ell}_0^{(2)} = 1.72$. Hence, the corresponding likelihood ratio statistic results in $\Lambda^{(2,1)} = -2 \cdot \left(\hat{\ell}_0^{(2)} - \hat{\ell}_1^{(1)}\right) = -2 \cdot (1.72 - 4.34) = 5.25$. In this case, under the null hypothesis $H_0^{(2)}$, the test statistic $\Lambda^{(2,1)}$ is approximately distributed as a chi-square random variable with $25 - 17 = 8$ dof. The corresponding p-value is $p^{(2,1)} = 0.731$, thus indicating that the null hypothesis $H_0^{(1)}$ can not be rejected at any plausible significance level.

To refine the analysis, the (currently) accepted hypothesis that only the parameters α_1, β_2, and σ_0 are unit-specific, now referred to as $H_1^{(2)}$, is tested against the following three null hypotheses:

- $H_0^{(3)}$: only α_1 and β_2 are unit-specific,
- $H_0^{(4)}$: only α_1 and σ_0 are unit-specific,
- $H_0^{(5)}$: only β_2 and σ_0 are unit-specific.

Also in this case the parameters under the above null hypotheses have been estimated, and the corresponding estimated log-likelihoods are $\hat{\ell}_0^{(3)} = -23.87$, $\hat{\ell}_0^{(4)} = -1.58$, and $\hat{\ell}_0^{(5)} = -21.53$. Obviously, the estimated log-likelihood under the alternative hypothesis $H_1^{(2)}$ is $\hat{\ell}_1^{(2)} = \hat{\ell}_0^{(2)} = 1.72$. The likelihood ratio statistics result in $\Lambda^{(3,2)} = 51.18$, $\Lambda^{(4,2)} = 6.60$, and $\Lambda^{(5,2)} = 46.50$, respectively. All these three test statistics, under the respective null hypotheses, are approximately distributed as chi-square random variables with $17 - 13 = 4$ dof. The resulting p-values, say $p^{(3,2)} = 2 \cdot 10^{-10}$, $p^{(4,2)} = 0.159$, and $p^{(5,2)} = 2 \cdot 10^{-9}$, show that only the null hypothesis $H_0^{(4)}$ that α_1 and σ_0 are unit-specific can not be rejected at any plausible significance level.

Thus, as further step, the currently accepted hypothesis that only α_1 and σ_0 are unit-specific, now referred as $H_1^{(3)}$, is tested against the following null hypotheses:

- $H_0^{(6)}$: only α_1 is unit-specific,
- $\mathrm{H}_0^{(7)}$: only σ_0 is unit-specific.

The corresponding estimated log-likelihoods are $\hat{\ell}_0^{(6)} = -25.48$, $\hat{\ell}_0^{(7)} = -22.50$, whereas of course $\hat{\ell}_1^{(3)} = \hat{\ell}_0^{(4)} = -1.58$. The likelihood ratio statistics result in $\Lambda^{(6,3)} = 47.79$ and $\Lambda^{(7,3)} = 41.84$. Both these test statistics, under the related null hypotheses, are approximately distributed as chi-square random variables with $13 - 9 = 4$ dof. The resulting p-values, $p^{(6,3)} = 1 \cdot 10^{-9}$ and $p^{(7,3)} = 2 \cdot 10^{-8}$, show that the null hypotheses $H_0^{(6)}$ and $H_0^{(7)}$ must be rejected at any plausible significance level.

Thus, this preliminary analysis carried out by using the original parameterization (1)–(2), whose results are summarized in Table A2, allows us to conclude that the proposed WP where only the parameters α_1 and σ_0 are unit-specific can be used to describe the observed MOSFET data in Table 1.

To complete this preliminary investigation, we also consider the alternative parameterization (10) of the proposed WP process. We then apply the model (10) to the whole set of data under the assumption that all the parameters

TABLE A3 ML estimates of the parameters $\mu, \alpha, \beta_1, \beta_2$, and σ of the reparametrized model and their coefficient of variation under the hypothesis that all parameters are unit-specific

	Unit i					
	1	**2**	**3**	**4**	**5**	***CV***
$\hat{\mu}$	0.0918	0.0934	0.1565	0.0506	0.1570	0.42
$\hat{\beta}_1$	0.5240	0.4804	0.3978	0.4709	0.3455	0.16
$\hat{\alpha}$	36,949	25,168	27,992	25,455	30,383	0.17
$\hat{\beta}_2$	20.822	7.437	8.625	9.359	11.067	0.47
$\hat{\sigma}$	0.094	0.101	0.118	0.134	0.381	0.73

are unit-specific. The ML estimates of the parameters $\mu, \alpha, \beta_1, \beta_2$, and σ are reported in Table A3. These estimates can be readily obtained from the estimates given in Table A1 by using the invariance property of ML estimators. For the same reason, the estimated log-likelihood under this alternative parameterization coincides with $\hat{\ell}_1^{(1)}$ and is equal to 4.34.

Based on the *CV* values given in the last column of Table A3, and by following the same semi-heuristic rule used for the original parameterization, we have applied the likelihood ratio test to check whether the WP where only the parameters μ, β_2, and σ (i.e., those with the highest *CV* values) are unit-specific should be preferred to the one that assumes that all the parameters are unit-specific. The tested hypotheses are then the following:

- null hypothesis $H_0^{(8)}$: only μ, β_2, and σ are unit-specific,
- alternative hypothesis $H_1^{(4)}$: all parameters are unit-specific.

Note that, due to the invariance property of the ML estimators, the hypothesis $H_1^{(4)}$ is equivalent to $H_1^{(1)}$. Under the null hypothesis $H_0^{(8)}$, the test statistic $\Lambda^{(8,4)} = -2 \cdot \left(\hat{\ell}_0^{(8)} - \hat{\ell}_1^{(4)}\right)$ is approximately distributed as a chi-square random variable with $25 - 17 = 8$ dof. The model parameters under the null hypothesis $H_0^{(8)}$ have been estimates and the corresponding estimated log-likelihood is $\hat{\ell}_0^{(8)} = 1.55$. Of course, $\hat{\ell}_1^{(4)} = \hat{\ell}_1^{(1)} = 4.34$, and hence $\Lambda^{(8,4)} = 5.58$. Because the corresponding *p*-value is $p^{(8,4)} = 0.694$, the null hypothesis $H_0^{(8)}$ that only the μ, β_2, and σ are unit-specific can not be rejected at any plausible significance level.

Hence, we have applied again the likelihood ratio test for checking the null hypothesis $H_0^{(8)}$ that only α_1, β_2, and σ are unit-specific, now referred to as hypothesis $H_1^{(5)}$, against the following null hypotheses:

- $H_0^{(9)}$: only μ and β_2 are unit-specific,
- $H_0^{(10)}$: only μ and σ are unit-specific,
- $H_0^{(11)}$: only β_2 and σ are unit-specific.

The ML estimates of the corresponding log-likelihoods are $\hat{\ell}_0^{(9)} = -13.85$, $\hat{\ell}_0^{(10)} = -7.58$, $\hat{\ell}_0^{(11)} = -22, 25$. Of course, $\hat{\ell}_0^{(8)} = \hat{\ell}_1^{(5)} = 1.55$. The corresponding likelihood ratio test statistics are then equal to $\Lambda^{(9,5)} = 30.80$, $\Lambda^{(10,5)} = 18.26$, and $\Lambda^{(11,5)} = 47.60$, respectively. Under the above null hypotheses the likelihood ratio test statistic is always approximately distributed as a chi-square random variable with $17 - 13 = 4$ dof. The corresponding *p*-values, say $p^{(9,5)} = 3 \cdot 10^{-6}$, $p^{(10,5)} = 1 \cdot 10^{-3}$, and $p^{(11,5)} = 1 \cdot 10^{-9}$, lead to reject the three null hypotheses at any plausible significance level. The testing results relative to the alternative parameterization (10) of the proposed WP are summarized in Table A4.

A further comparison between the best model under the original parameterization (1)–(2), that is a WP where only α_1 and σ_0 are unit-specific and the best model under the alternative parameterization (10), that is a WP where μ, β_2, and σ are unit-specific, is then performed by using the Akaike Information Criterion. On the basis of the estimated log-likelihoods, the AIC value relative to the best model under the original parametrization (1)–(2) is equal to 29.16, whereas the AIC value relative to the best model under the alternative parametrization (10) is equal to 30.90.

Thus, according to the results of the likelihood ratio tests and of the Akaike Information Criterion, the model that will be used to describe the degradation paths of the five MOSFETs is the WP (1) with mean function (2), where the only

TABLE A4 Likelihood ratio test results relative to MOSFET data, under the alternative parameterization

Null hypothesis H_0	Alternative hypothesis H_1	Λ	dof	p-value	Decision
Only μ, β_2, and σ are unit-specific	All parameters are unit-specific	5.58	8	0.694	Not reject H_0
Only μ and β_2 are unit-specific	μ, β_2, and σ are unit-specific	30.80	4	$3 \cdot 10^{-6}$	Reject H_0
Only μ and σ are unit-specific	μ, β_2, and σ are unit-specific	18.26	4	$1 \cdot 10^{-3}$	Reject H_0
Only β_2 and σ are unit-specific	μ, β_2, and σ are unit-specific	47.60	4	$1 \cdot 10^{-9}$	Reject H_0

TABLE A5 ML estimates of the process parameters under the hypothesis that only the values of α_1 and σ_0 are unit-specific

	Unit i				
	1	2	3	4	5
$\hat{\alpha}_1$ (sec)	51.6	114.2	231.7	526.3	739.6
$\hat{\beta}_1$			0.4652		
$\hat{\alpha}_2$ (sec)			35,449		
$\hat{\beta}_2$			8.389		
$\hat{\sigma}_0$	0.342	0.330	0.311	0.601	0.977

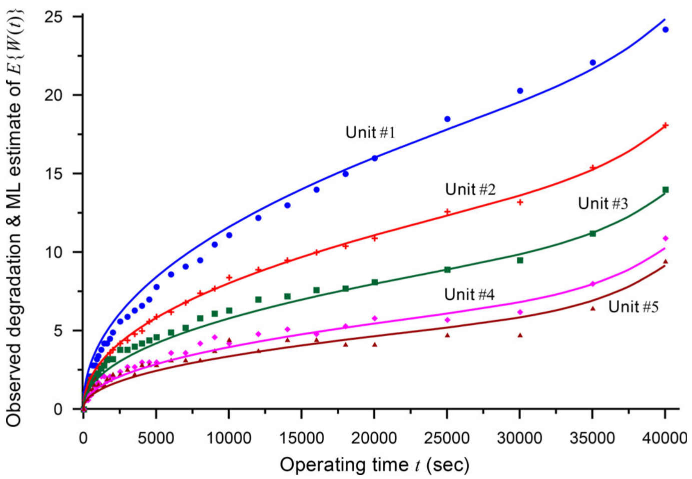

FIGURE A3 Observed degradation data (dots) and ML estimate of $E\{W(t)\}$ of each unit (solid lines) where only the parameters α_1 and σ_0 are unit-specific

parameters that are unit-specific are α_1 and σ_0. The corresponding ML estimates of the process parameters are given in Table A5.

In Figure A3 the observed degradation data are plotted together to the ML estimates of the mean degradation function $E\{W(t)\}$ of the five MOSFETs, obtained by computing (unit-by-unit) the function (2) at the ML estimates reported in Table A5. The plot shows that the proposed WP with common parameters β_1, α_2, and β_2, and only α_1 and σ_0 unit-specific, fits well the observed degradation paths.